

1 **Coccolithophore populations and their contribution to carbonate export during an**  
2 **annual cycle in the Australian sector of the Antarctic Zone**

3 Andrés S. Rigual Hernández<sup>1,\*</sup>, José A. Flores<sup>1</sup>, Francisco J. Siirro<sup>1</sup>, Miguel A. Fuertes<sup>1</sup>,  
4 Lluïsa Cros<sup>2</sup> and Thomas W. Trull<sup>3,4</sup>

5 1 Área de Paleontología, Departamento de Geología, Universidad de Salamanca, 37008  
6 Salamanca, Spain

7 2 Institut de Ciències del Mar, CSIC, Passeig Marítim 37-49, 08003 Barcelona, Spain.

8 3 Antarctic Climate and Ecosystems Cooperative Research Centre, University of  
9 Tasmania, Hobart, Tasmania 7001, Australia

10 4 CSIRO Oceans and Atmosphere Flagship, Hobart, Tasmania 7001, Australia

11 \*corresponding author

12 Email: arigual@usal.es

13 **Abstract**

14 The Southern Ocean is experiencing rapid and relentless change in its physical and  
15 biogeochemical properties. The rate of warming of the Antarctic Circumpolar Current  
16 exceeds that of the global ocean, and the enhanced uptake of carbon dioxide is causing  
17 basin-wide ocean acidification. Observational data suggest that these changes are  
18 influencing the distribution and composition of pelagic plankton communities. Long-term  
19 and annual field observations on key environmental variables and organisms are a critical  
20 basis for predicting changes in Southern Ocean ecosystems. These observations are  
21 particularly needed, since high-latitude systems have been projected to experience the  
22 most severe impacts of ocean acidification and invasions of allochthonous species.

23 Coccolithophores are the most prolific calcium carbonate producing phytoplankton  
24 group, playing an important role in Southern Ocean biogeochemical cycles. Satellite  
25 imagery has revealed elevated particulate inorganic carbon concentrations near the major  
26 circumpolar fronts of the Southern Ocean, that can be attributed to the coccolithophore  
27 *Emiliania huxleyi*. Recent studies have suggested changes during the last decades in the  
28 distribution and abundance of Southern Ocean coccolithophores. However, due to limited  
29 field observations, the distribution, diversity and state of coccolithophore populations in  
30 the Southern Ocean remain poorly characterised.

31 We report here on seasonal variations in the abundance and composition of  
32 coccolithophore assemblages collected by two moored sediment traps deployed at the  
33 Antarctic Zone south of Australia (2000 and 3700 m depth) for one year in 2001-02.  
34 Additionally, seasonal changes in coccolith weights of *E. huxleyi* populations were  
35 estimated using circularly polarised micrographs analysed with *C-Calcita* software. Our  
36 findings indicate that (1) coccolithophore sinking assemblages were nearly monospecific  
37 for *E. huxleyi* morphotype B/C in the Antarctic Zone waters in 2001-2002; (2) coccoliths  
38 captured by the traps experienced weight and length reduction during summer (December  
39 – February); (3) the estimated annual coccolith weight of *E. huxleyi* at both sediment traps  
40 ( $2.11 \pm 0.96$  and  $2.13 \pm 0.91$  pg at 2000 m and 3700 m) was consistent with previous  
41 studies for morphotype B/C in other Southern Ocean settings (Scotia Sea and Patagonian  
42 shelf); (4) coccolithophores accounted for approximately 2-5% of the annual, deep-ocean  
43 CaCO<sub>3</sub> flux. Our results are the first annual record of coccolithophore abundance,  
44 composition and degree of calcification in the Antarctic Zone. They provide a baseline  
45 against which to monitor coccolithophore responses to changes in environmental  
46 conditions expected for this region in coming decades.

47

48 **Key words:** Southern Ocean, Antarctic Zone, coccolithophores, coccolith weight,  
49 sediment traps.

50

## 51 **1. Introduction**

### 52 **1.1. Background and objectives**

53 The rapid increase in atmospheric CO<sub>2</sub> levels since the onset of the industrial  
54 revolution is modifying the environmental conditions of marine ecosystems in a variety  
55 of ways. The enhanced greenhouse effect, mainly driven by increased atmospheric CO<sub>2</sub>  
56 levels, is causing ocean warming (Barnett et al., 2005), shallowing of mixed layer depths  
57 (Levitus et al., 2000) and changes in light penetration and nutrient supply (Bopp et al.,  
58 2001; Rost and Riebesell, 2004; Sarmiento et al., 2004b; Deppeler and Davidson, 2017).  
59 Moreover, the enhanced accumulation of CO<sub>2</sub> in the ocean is giving rise to changes in the  
60 ocean carbonate system, including reduction of carbonate ion concentrations and  
61 lowering of seawater pH. Most evidence suggests that the ability of many marine  
62 calcifying organisms to form carbonate skeletons and shells may be reduced with  
63 increasing seawater acidification including some species of (but not all) coccolithophores,

64 corals, pteropods and foraminifera (e.g. Orr et al., 2005; Moy et al., 2009; Lombard et al.,  
65 2010; Beaufort et al., 2011; Andersson and Gledhill, 2013). Since phytoplankton are  
66 extremely sensitive to global environmental change (Litchman et al., 2012) all predicted  
67 changes in marine environmental conditions are likely to modify the abundance,  
68 composition and distribution of phytoplankton communities.

69 Changes in the relative abundances of major phytoplankton functional groups are  
70 likely to influence ocean biogeochemistry and ocean carbon storage, with feedbacks to  
71 the rate of climate change (e.g. Boyd and Newton, 1995; Boyd et al., 1999; Falkowski et  
72 al., 2004; Cermeño et al., 2008). The precipitation and sinking of  $\text{CaCO}_3$  by  
73 coccolithophores has the potential for complex contributions to carbon cycling.  
74 Carbonate precipitation removes more alkalinity than dissolved inorganic carbon from  
75 surface waters, thereby acting to increase  $\text{pCO}_2$  in surface waters (the so-called carbonate  
76 counter pump, e.g. Zeebe, (2012)). On the other hand, ballasting by carbonates appears  
77 to increase transfer of organic carbon to the ocean interior (Armstrong et al., 2002; Klaas  
78 and Archer, 2002). On seasonal timescales the counter pump contribution dominates  
79 (Boyd and Trull, 2007), but more complex interactions can occur over longer timescales  
80 as a result of changing extents of carbonate dissolution in sediments, including the  
81 possibility that enhanced calcite dissolution in the Southern Ocean contributed to lower  
82 atmospheric  $\text{CO}_2$  levels during glacial maxima (Archer and Maier-Reimer, 1994; Sigman  
83 and Boyle, 2000; Ridgwell and Zeebe, 2005).

84 The Southern Ocean is a critical component of the Earth's ocean–climate system  
85 and plays a pivotal role in the global biogeochemical cycles of carbon and nutrients  
86 (Sarmiento et al., 2004a; Anderson et al., 2009). Despite the fact that the Southern Ocean  
87 accounts for about 25% of the global ocean, it contains ~40% of the global ocean  
88 inventory of anthropogenic  $\text{CO}_2$  (Khatiwala et al., 2009; Takahashi et al., 2009; Frölicher  
89 et al., 2015), and it exports nutrients to more northern latitudes ultimately supporting ~  
90 75% of the ocean primary production north of  $30^\circ\text{S}$  (Sarmiento et al., 2004a). Model  
91 projections suggest that the reduction in the saturation state of  $\text{CaCO}_3$  will reach critical  
92 thresholds sooner in cold, high-latitude ecosystems such as the Southern Ocean (Orr et  
93 al., 2005; McNeil and Matear, 2008; Feely et al., 2009). Therefore, calcifying organisms  
94 living in these regions will be the first to face the most severe impacts of ocean  
95 acidification.

96 In view of the rapid changes in climate and other environmental stressors presently  
97 occurring in the Southern Ocean, a major challenge facing the scientific community is to

98 predict how phytoplankton communities will reorganise in response to global change. In  
99 this regard, two main aspects of the distributions of coccolithophores are emerging.  
100 Firstly, coccolithophores exhibit high concentrations in the Subantarctic Southern Ocean,  
101 a feature termed by Balch et al. (2011) as the “Great Calcite Belt” based on satellite  
102 reflectance estimates of PIC abundances. Although importantly the PIC accumulations  
103 are significantly less than those that arise in the North Atlantic, and the satellite algorithm  
104 is not reliable in Antarctic waters, where it badly overestimates PIC abundances (Balch  
105 et al., 2016; Trull et al., 2017). Secondly, recent studies suggest that the magnitude and  
106 geographical distribution of *E. huxleyi* blooms may be experiencing significant and rapid  
107 changes. Cubillos et al. (2007) and Winter et al. (2014) postulated that *E. huxleyi* has  
108 expanded its ecological niche south of the Polar Front in the recent decades.  
109 Contrastingly, Freeman and Lovenduski (2015) suggested an overall decline in Southern  
110 Ocean PIC concentrations using satellite records between 1998 and 2014. The  
111 explanation of these contrasting results may lie in the methodologies applied. While  
112 shipboard surface water observations provide a highly detailed picture of a given  
113 ecosystem, they are very sparse, only represent a snapshot in time, and can easily miss  
114 blooms of any given species. The satellite PIC signal has the great advantage of largescale  
115 and repeated coverage, but can miss subsurface populations (e.g. Winter et al., 2014) and  
116 be mimicked by the spectral characteristics of other scattering sources. The most  
117 important among them are probably microbubbles (Zhang et al., 2002), glacial flour  
118 (Balch et al., 2011) and noncalcifying organisms such as *Phaeocystis antarctica* (Winter  
119 et al., 2014), a colonial prymnesiophyte algae very abundant in high latitude systems of  
120 the Southern Ocean (e.g. Arrigo et al., 1999; Arrigo et al., 2000). Notably the PIC  
121 algorithm performs particularly poorly in Antarctic waters (Balch et al., 2016; Trull et al.,  
122 2017)

123 For these reasons, year-round field observations of areas representative of key  
124 Southern Ocean regions are essential to determine the current state of coccolithophore  
125 communities and to develop baselines against which long-term trends can be detected.  
126 Moreover, a better understanding of coccolithophore distribution, ecology and seasonal  
127 dynamics is required to improve our interpretations of the sedimentary record and our  
128 models of biogeochemistry. Sediment traps are a direct method to collect data about  
129 calcareous and siliceous micro and nanoplankton. Traps allow the monitoring of seasonal  
130 and annual variability of plankton export, document species successions, and help to  
131 determine the specific role of microplankton species in the biological and carbonate

132 pumps. The autonomous collection capacity of sediment traps is particularly useful in the  
133 remote Southern Ocean, where inaccessibility and harsh working conditions prevent year-  
134 round ship-based sampling.

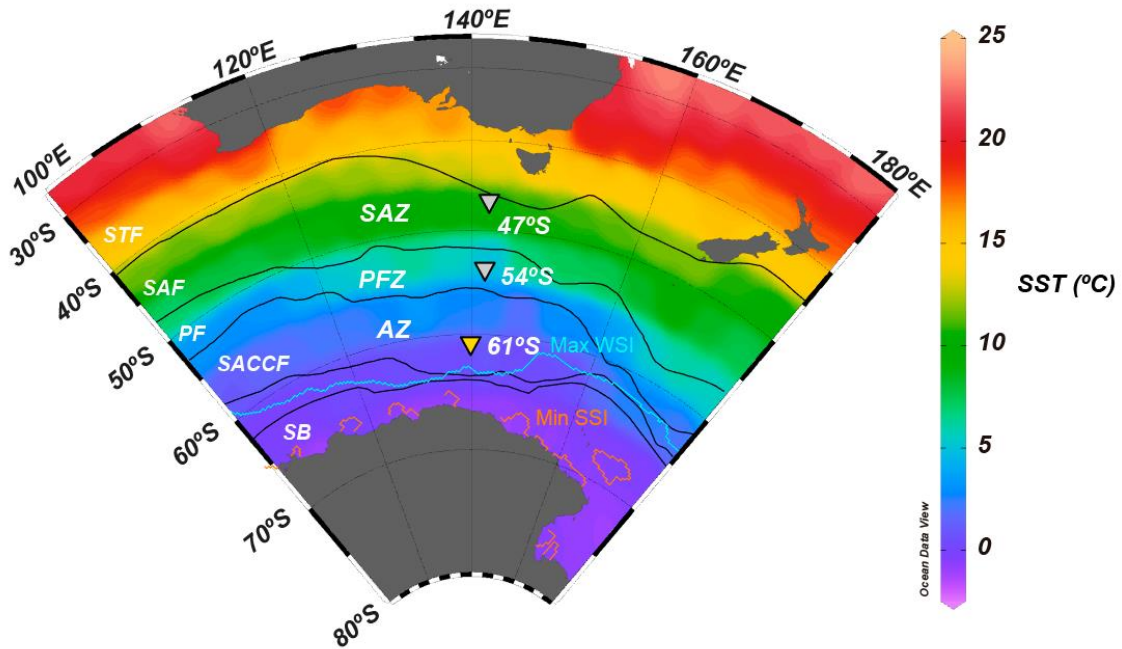
135 We present here the first record of composition, abundance, and seasonality of  
136 coccolithophore assemblages in the Antarctic Zone of the Southern Ocean, collected by  
137 two deep ocean sediment traps deployed on a single mooring during 10 months south of  
138 Australia at the site of the Southern Ocean Iron Release Experiment (SOIREE) near 61°S,  
139 140°E (Boyd et al., 2000a). Moreover, we report weight and length measurements on *E.*  
140 *huxleyi* coccoliths, assessing the impact of seasonally varying environmental parameters  
141 on *E. huxleyi* coccoliths. That provides a baseline of coccolith dimensions for the  
142 populations living in this region. All the above information is needed for monitoring  
143 coccolithophore responses, if any, to changing environmental conditions in the Antarctic  
144 Zone south of Australia during coming decades.

145

## 146 **1.2 Regional setting and oceanography**

147 The southern Antarctic Zone (AZ-S; Parslow et al., 2001) is delimited in the north  
148 by the southern branch of the Polar Front (PF) and in the south by the southern front of  
149 the Antarctic Circumpolar Current (SACCF) (Fig. 1). Trull et al. (2001b) summarised the  
150 seasonal evolution of water column properties in the study region. The intense heat loss  
151 of surface waters during winter decreases Sea Surface Temperature (SST) to values <  
152 1°C, resulting in strong vertical convection. Winter mixing extends to depths of about  
153 120 m, replenishing the upper water column with nutrients. Chlorophyll-*a* levels during  
154 winter are negligible throughout the region due to the reduced solar radiation and the  
155 deep, continuous vertical mixing. During summer, increasing solar radiation warms the  
156 surface ocean and a seasonal thermocline forms (Fig. 2). By late summer-early autumn  
157 (March) SST ranges between 2 and 3 °C. Considerable nutrient depletion associated with  
158 a moderate increase in algal biomass occurs within the mixed layer (Trull et al., 2001b).  
159 Nonetheless, due to the limited sampling of the study region, the timing of the summer  
160 nutrient minimum is not well constrained by the available data (Trull et al., 2001b).  
161 Silicate exhibits the strongest summer draw-down of all the macronutrients, reaching  
162 ~30% of its winter values (Fig. 2; Trull et al., 2001b), mainly due to diatom growth and  
163 subsequent biogenic silica export to the deep sea (Rigual-Hernández et al., 2015a). The  
164 low algal biomass accumulation in the region is attributed to the very low iron levels (0.1-

165 0.2 nM; Boyd et al., 2000a; Sohrin et al., 2000). Mesozooplankton analysis during the  
 166 SOIREE experiment by Zeldis (2001) indicates that zooplankton community in the study  
 167 region is dominated by copepods. Grazing pressure was low (<1% of the phytoplankton  
 168 standing stock removed per day) and, therefore, is thought not to play an important role  
 169 in the control of the micro-phytoplankton (primarily diatom) stocks, but nanoflagellate  
 170 grazer abundances were significant and were likely to have regulated smaller

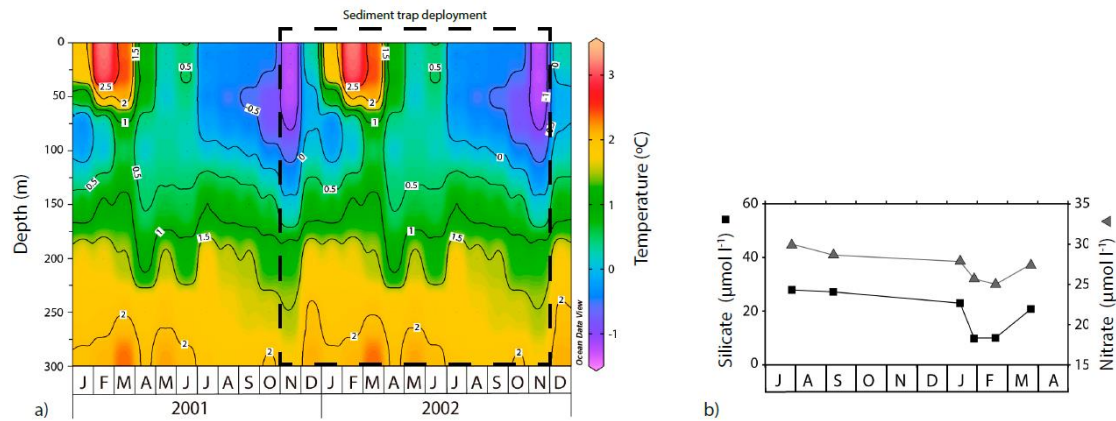


171 phytoplankton abundances (Hall and Safi, 2001).

172

173 **Figure 1.** Annual mean sea surface temperature map (World Ocean Atlas; Locarnini et  
 174 al., 2013) of the Australian sector of the Southern Ocean, showing the position of the  
 175 main frontal and zonal systems (adapted from Orsi et al., 1995) and the location of the  
 176 61°S, 54°S and 47°S sediment trap stations (inverted triangles). Abbreviations: STF -  
 177 Subtropical Front, SAZ - Subantarctic Zone, SAF - Subantarctic Front, PFZ - Polar  
 178 Frontal Zone, PF - Polar Front, AZ - Antarctic Zone, SACCf - Southern Antarctic  
 179 Circumpolar Current Front, SB - Southern Boundary, Max WSI - Maximum Winter Sea  
 180 Ice Extent (August 2001) and Min SSI – Minimum Summer Sea Ice Extent (February  
 181 2002) (Fetterer et al., 2017).

182

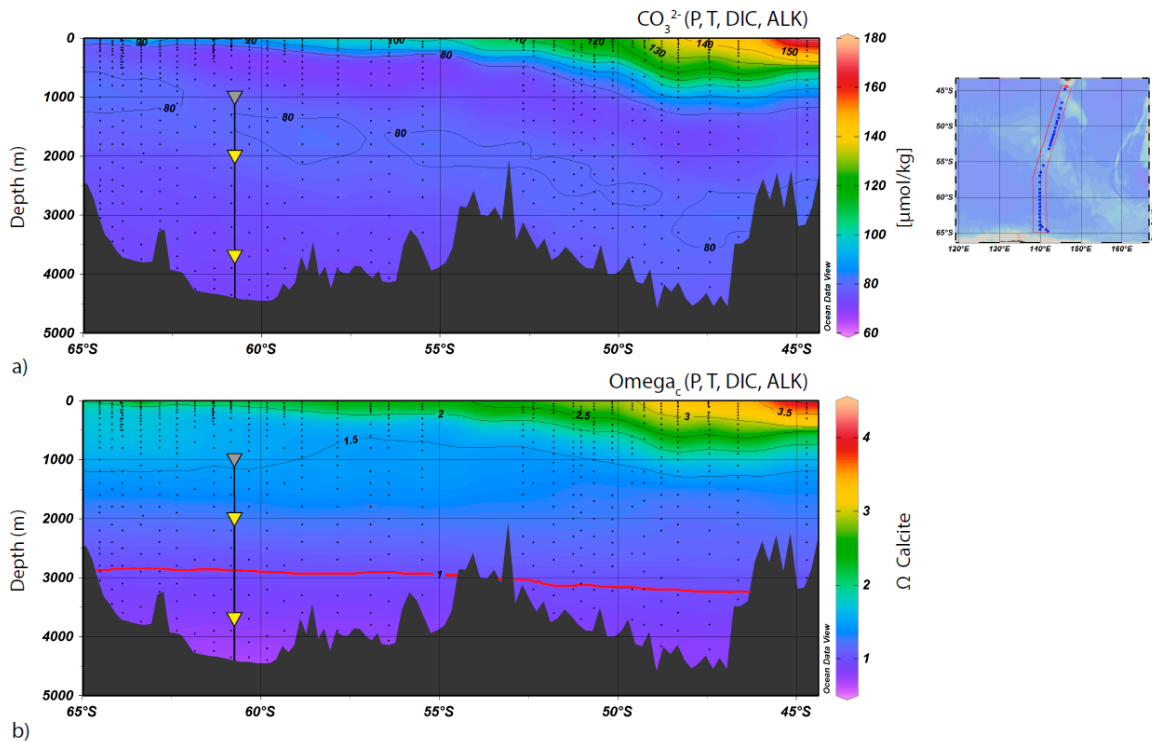


183

184 **Figure 2:** (a) Seasonal variation in the vertical structure of temperature (°C) between  
 185 January 2001 and December 2002 for the 61°S site from the World Ocean Atlas 2009  
 186 (Locarnini et al., 2010). (b) Summary of seasonal evolution of macronutrient  
 187 concentrations (silicate and nitrate) in the mixed layer at the 61°S site taken from the  
 188 WOCE SR3 transects between 1993 and 1996 (modified from Trull et al., 2001b) (b).

### 189 1.3 Water carbonate chemistry in the study region

190 Calcite solubility increases at higher pressures and lower temperatures, so that  
 191 dissolution increases with depth in the water column. Based on downward changes in the  
 192 calcite dissolution rate, two critical depth horizons can be distinguished: the Calcite  
 193 Saturation Horizon (CSH) that can be defined as the depth at which the water becomes  
 194 undersaturated with respect to calcite (i.e. where  $\Omega_{\text{calcite}} = 1$ ); and the  $\text{CaCO}_3$   
 195 compensation depth (CCD), the depth at which the rate of calcite rain from the upper  
 196 water column equals the dissolution rate. Figure 3 shows carbonate concentrations [ $\text{CO}_3^{2-}$   
 197 ] and calcite saturation ( $\Omega_{\text{calcite}}$ ) for the WOCE SR03 2001 transect between Antarctica  
 198 and Tasmania along the 140°E meridian as estimated by Bostock et al. (2011). In the AZ-  
 199 S waters south of Tasmania, the CSH and CCD occur at 3000 and 3700 m, respectively  
 200 (Fig. 3). Therefore, the location of sediment traps at the 61°S site allows for the  
 201 assessment of dissolution changes, if any, of coccolithophore assemblages between the  
 202 two critical dissolution depth horizons: the CSH and CCD. Notably, both progressive  
 203 uptake of anthropogenic  $\text{CO}_2$  and increased upwelling of naturally  $\text{CO}_2$ -rich deep waters  
 204 over the past 20 years is leading to shallowing of these features (Pardo et al., 2017)



206

207 **Figure 3.** Cross section of the mooring location in comparison to regional seafloor  
 208 bathymetry, carbonate concentrations  $[CO_3^{2-}]$  and calcite saturation ( $\Omega_{\text{calcite}}$ ) for WOCE  
 209 transect SR03 2001 from Bostock et al. (2011), who calculated them from the Dissolved  
 210 Inorganic Carbon (DIC) and alkalinity in the CARINA database (CARINA, 2011). The  
 211 location of the transects is shown on the map on the right top.  $\Omega_{\text{calcite}} = 1$  contour is  
 212 highlighted with a red line to show the approximate depth of the CSH across the transect.

213

## 214 2. Material and Methods

### 215 2.1 Sediment trap experiment

216 As part of the SAZ collaborative research program (Trull et al., 2001c), a sediment  
 217 trap experiment was carried out at the 61°S site (60° 44.43'S; 139° 53.97'E) in the  
 218 Australian sector of the southern Antarctic Zone within the region where the Southern  
 219 Ocean Iron Release Experiment (SOIREE) was conducted (Boyd et al., 2000a). The 61°S  
 220 site is characterised by weak currents with a mean eastward geostrophic surface velocity  
 221 of approximately  $0.03 \pm 0.02 \text{ m s}^{-1}$  (Trull et al., 2001b). The site is north of the Seasonal  
 222 Sea-Ice Zone (Massom et al., 2013; Rigual-Hernández et al., 2015a) and remote from any  
 223 known iceberg pathway (Gladstone et al., 2001).

224 The mooring was equipped with three McLane Parflux time series sediment traps (Honjo  
225 and Doherty, 1988) for approximately one year (November 30, 2001 to September 29,  
226 2002, 317 days). The traps were located at 1000, 2000 and 3700 m below the surface in  
227 a water column of 4393 m (Figures 3a and 3b). Each trap was provided with 21 cups.  
228 Sampling intervals were synchronised between traps and in order to resolve the seasonal  
229 flux cycle ranged from 8 days (in austral summer) to 55 days in austral winter. No samples  
230 were recovered from the shallowest trap owing to equipment malfunction and, therefore,  
231 only results for the 2000 and 3700 m traps are presented here. Each trap was paired with  
232 an Aanderaa current meter and temperature sensors. The 250 ml collection cups were  
233 filled with a buffered solution of sodium tetraborate ( $1 \text{ g L}^{-1}$ ), sodium chloride ( $5 \text{ g L}^{-1}$ ),  
234 strontium chloride ( $0.22 \text{ g L}^{-1}$ ), and mercury chloride ( $3 \text{ g L}^{-1}$ ) in unfiltered, deep ( $> 1000$   
235 m) seawater from the region. Risk of sample contamination by the unfiltered seawater is  
236 considered negligible due to the fact that the deep water exhibits low particle abundance  
237 and also because particle concentration in sea water is of the order of  $\mu\text{g/L}$  while  
238 concentration in the trap cups after recovery was of the order of  $\text{mg/L}$ .

239 The two deeper traps completed their collection sequence as programmed,  
240 providing continuous time-series for a year. Due to the low particle fluxes during the  
241 winter, insufficient material remained for phytoplankton analysis of cup 1 from the 2000  
242 m trap and cups 1, 2, 19, 20 and 21 from the 3700 m trap (Table 1).

243

## 244 **2.2 Sample processing and coccolithophore counting procedure**

245

246 The sediment trap cup contents were washed through a 1 mm sieve after recovery  
247 and then divided into 10 aliquots using a rotary splitter (McLane, Inc.). A description of  
248 the analytical procedures for estimation of geochemical fluxes is provided in Trull et al.  
249 (2001a) and Rigual-Hernández et al. (2015a). One aliquot was used for siliceous and  
250 calcareous micro- and nano-plankton analyses. Each fraction for plankton analysis was  
251 refilled with distilled water to 40 ml, from which 10 ml was subsampled and buffered  
252 with a solution of sodium carbonate and sodium hydrogen carbonate (pH 8) and kept  
253 refrigerated for calcareous nannoplankton analysis. Samples for coccolithophore analysis  
254 were prepared following the methodology of Flores and Sierro (1997). In short, 300  $\mu\text{l}$   
255 were extracted with a micropipette and dropped onto a glass Petri dish previously filled  
256 with a buffered solution and with a cover slip on its bottom. After settling for 12 hours,  
257 the buffer solution was removed using short strips of filter paper placed at the edge of the

258 dish. Then, the cover slip was left to dry completely and mounted on a glass slide using  
259 Canada balsam. Coccoliths were identified and counted using a Nikon Eclipse 80i  
260 polarised light microscope at 1000× magnification. A minimum of 400 coccoliths were  
261 counted in each sample. Coccospheres occurred in much lower numbers than loose  
262 coccoliths in these preparations. The coccolith counts were transformed into daily fluxes  
263 of specimens  $\text{m}^{-2} \text{d}^{-1}$  following the formula:

264

$$265 \quad F = \frac{N \times \frac{A}{n \times a} \times V \times S}{d \times T}$$

266

267 where “ $F$ ” is the daily coccolith flux, “ $N$ ” the number of coccoliths, “ $A$ ” the total area of  
268 a Petri dish, “ $n$ ” the number of fields-of-view analysed, “ $a$ ” the area of a single field of  
269 view, “ $V$ ” the dilution volume, “ $S$ ” the split of the cup, “ $d$ ” the number of days of  
270 collection and “ $T$ ” the aperture area of the sediment trap.

271 Since the sediment trap collection period was shorter than a full calendar year, an  
272 estimate of the annual coccolith flux of the 2000 m trap was calculated. This estimate  
273 takes into account the fact that the unsampled days occurred in winter when particle fluxes  
274 were low, and were obtained using the flux for the last winter cup (#21 in 2002) to  
275 represent mean daily fluxes during the unobserved interval. Due to the lack of samples  
276 corresponding to winter 2002 for the 3700 m sediment trap record, the annualization of  
277 the coccolith fluxes for this trap was made based only on the samples with available data.  
278 Therefore, the annualised and annual flux data for the 3700 m trap presented in Table 1  
279 should be used with caution.

61_2000		Sampling period	Length	Total Mass Flux	CaCO <sub>3</sub>			POC		Diatoms	Coccolithophore flux	Relative abundance		
Cup	mid point	days	mg m <sup>-2</sup> d <sup>-1</sup>	mg m <sup>-2</sup> d <sup>-1</sup>	%	mg m <sup>-2</sup> d <sup>-1</sup>	%	10 <sup>6</sup> valves m <sup>-2</sup> d <sup>-1</sup>	10 <sup>6</sup> coccoliths m <sup>-2</sup> d <sup>-1</sup>	<i>E. huxleyi</i>	<i>C. leptoporus</i>	Other		
1	nov. 30, 2001	8	48	14	30	0.7	1.5	-	-	-	-	-		
2	dic. 08, 2001	8	78	17	22	1.7	2.2	9	2.5	98.8	1.2	0.0		
3	dic. 16, 2001	8	326	62	19	6.9	2.1	82	2.7	98.5	1.3	0.2		
4	dic. 24, 2001	8	509	140	28	6.4	1.3	85	8.2	99.5	0.5	0.0		
5	ene. 01, 2002	8	1151	44	4	26.9	2.3	408	12.3	99.8	0.2	0.0		
6	ene. 09, 2002	8	1069	170	16	14.8	1.4	200	22.3	99.8	0.2	0.0		
7	ene. 17, 2002	8	656	60	9	11.3	1.7	159	9.2	99.3	0.7	0.0		
8	ene. 25, 2002	8	702	38	5	11.0	1.6	296	8.4	99.3	0.7	0.0		
9	feb. 02, 2002	8	666	39	6	12.0	1.8	184	5.4	98.8	1.2	0.0		
10	feb. 10, 2002	8	595	24	4	8.2	1.4	295	6.0	99.5	0.5	0.0		
11	feb. 18, 2002	8	534	20	4	6.2	1.2	149	9.8	99.0	0.5	0.5		
12	feb. 26, 2002	8	524	19	4	4.7	0.9	152	5.0	100.0	0.0	0.0		
13	mar. 06, 2002	8	586	15	3	6.9	1.2	120	6.4	99.8	0.2	0.0		
14	mar. 14, 2002	8	285	11	4	3.2	1.1	71	2.0	99.8	0.2	0.0		
15	mar. 22, 2002	8	290	7	3	3.2	1.1	66	2.0	97.6	1.0	1.5		
16	mar. 30, 2002	8	263	8	3	2.6	1.0	87	0.9	99.2	0.8	0.0		
17	abr. 08, 2002	10	264	7	3	2.2	0.8	97	1.3	98.1	1.9	0.0		
18	may. 08, 2002	50	130	5	4	1.2	1.0	47	0.8	99.8	0.2	0.0		
19	jun. 29, 2002	54	65	2	4	0.7	1.0	10	0.7	98.8	0.8	0.4		
20	ago. 22, 2002	55	56	2	4	0.8	1.5	19	0.9	99.5	0.2	0.2		
21	sep. 29, 2002	20	42	2	4	0.5	1.3	6	0.9	98.0	2.0	0.0		
Annualised values			232	17	7.4	3.3	1.4	67	2.8					
Annual flux			85 g m <sup>-2</sup> y <sup>-1</sup>	6 g m <sup>-2</sup> y <sup>-1</sup>		1.2 g m <sup>-2</sup> y <sup>-1</sup>		24 10 <sup>8</sup> valves m <sup>-2</sup> y <sup>-1</sup>	1.03 10 <sup>11</sup> coccoliths m <sup>-2</sup> y <sup>-1</sup>	99.4	0.5	0.1		

61_3700		Sampling period	Length	Total Mass Flux	CaCO <sub>3</sub>			POC		Diatoms	Coccolithophore flux	Relative abundance		
Cup	mid point	days	mg m <sup>-2</sup> d <sup>-1</sup>	mg m <sup>-2</sup> d <sup>-1</sup>	%	mg m <sup>-2</sup> d <sup>-1</sup>	%	10 <sup>6</sup> valves m <sup>-2</sup> d <sup>-1</sup>	10 <sup>7</sup> coccoliths m <sup>-2</sup> d <sup>-1</sup>	<i>E. huxleyi</i>	<i>C. leptoporus</i>	Other		
1	nov. 30, 2001	8	38	9	23	0.4	1.1	-	-	-	-	-		
2	dic. 08, 2001	8	31	9	28	0.4	1.2	-	-	-	-	-		
3	dic. 16, 2001	8	99	29	30	1.4	1.4	4	1.3	99.0	0.7	0.2		
4	dic. 24, 2001	8	231	59	26	1.4	0.6	12	5.5	99.3	1.5	0.2		
5	ene. 01, 2002	8	873	87	10	17.3	2.0	118	11.6	99.8	0.2	0.0		
6	ene. 09, 2002	8	1157	154	13	19.8	1.7	479	15.9	100.0	0.0	0.0		
7	ene. 17, 2002	8	828	166	20	9.4	1.1	354	20.0	100.0	0.0	0.0		
8	ene. 25, 2002	8	490	34	7	6.4	1.3	169	11.0	99.8	0.2	0.0		
9	feb. 02, 2002	8	491	32	6	6.5	1.3	385	4.6	100.0	0.0	0.0		
10	feb. 10, 2002	8	419	19	4	6.0	1.4	281	4.2	99.8	0.2	0.0		
11	feb. 18, 2002	8	584	36	6	6.2	1.1	254	15.9	99.1	0.7	0.2		
12	feb. 26, 2002	8	581	31	5	5.2	0.9	238	12.2	100.0	0.0	0.0		
13	mar. 06, 2002	8	849	23	3	7.6	0.9	326	15.0	99.8	0.2	0.0		
14	mar. 14, 2002	8	369	18	5	3.3	0.9	44	6.6	99.2	0.8	0.0		
15	mar. 22, 2002	8	218	8	4	2.6	1.2	32	6.6	99.5	0.2	0.2		
16	mar. 30, 2002	8	258	10	4	2.5	1.0	43	6.8	99.3	0.7	0.0		
17	abr. 08, 2002	10	257	9	3	2.3	0.9	32	4.8	99.5	0.2	0.2		
18	may. 08, 2002	50	118	5	4	1.2	1.0	8	1.2	99.8	0.0	0.2		
19	jun. 29, 2002	54	0	0	4	0.0	1.0	-	-	-	-	-		
20	ago. 22, 2002	55	0	0	4	0.0	1.0	-	-	-	-	-		
21	sep. 29, 2002	20	0	0	4	0.0	1.0	-	-	-	-	-		
Annualised values			188	17	9	2.3	1.2	62	3.3					
Annual flux			69 g m <sup>-2</sup> y <sup>-1</sup>	6 g m <sup>-2</sup> y <sup>-1</sup>		0.9 g m <sup>-2</sup> y <sup>-1</sup>		23 10 <sup>8</sup> valves m <sup>-2</sup> y <sup>-1</sup>	1.20 10 <sup>11</sup> coccoliths m <sup>-2</sup> y <sup>-1</sup>	99.7	0.2	0.1		

280 **Table 1:** Daily export fluxes of total mass flux, calcium carbonate (CaCO<sub>3</sub>), particulate  
281 organic carbon (POC), diatom valves and coccoliths registered at the 61°S site from  
282 November 2001 through October 2002. Mass fluxes listed as zero were too small to  
283 measure (<1 mg).

284

### 285 2.3 SEM analysis

286 As the resolution of the light microscope is insufficient to differentiate *E. huxleyi*  
287 morphotypes, the samples of the 2000 m trap record were analysed using a Scanning  
288 Electron Microscope (SEM). Glass cover-slips were prepared following the method  
289 outlined by Flores and Sierro (1997). The dried cover-slips were mounted on aluminium  
290 stubs and coated with gold. An EVO HD25 SEM (Carl Zeiss) was used to determine the  
291 morphotype of *E. huxleyi* coccoliths found in the samples (magnification 5000-20000x).  
292 Due to the large abundance of diatom valves and the scarcity of coccoliths in the samples,  
293 a compromise between number of identified coccoliths and time spent had to be reached.  
294 Therefore, a target minimum of thirty *E. huxleyi* coccoliths per sample were identified.  
295 The taxonomic concepts of Young and Westbroek (1991), Young et al. (2003), Cubillos

296 et al. (2007) and Hagino et al. (2011) were followed to classify the *E. huxleyi* coccoliths  
297 into different morphotypes.

298

#### 299 **2.4 C-*Calcita* analyses**

300 The glass slides used for coccolith counts were also analysed for coccolith mass  
301 and size measurements using a Nikon Eclipse LV100 POL polarised light microscope  
302 equipped with circular polarization and a Nikon DS-Fi1 8-bit colour digital camera.  
303 Calibration images were performed on an apical rhabdolith of the genus *Acanthoica*  
304 collected by a sediment trap at the 47°S site (46°48'S, 142°6'E), located in the Australian  
305 sector of the Subantarctic Zone. Camera parameters and microscope light settings were  
306 maintained constant throughout the imaging session. Depending on coccolith  
307 concentration, between 13-28 random fields of view per sample were photographed. The  
308 images were then analysed by the image processing software *C-*Calcita** (Fuertes et al.,  
309 2014). The output files for single *E. huxleyi* coccoliths were visually selected. Length and  
310 weight measurements were automatically performed by *C-*Calcita** software. A total of  
311 2328 coccoliths were analysed with a minimum of 50 coccoliths per sample. For more  
312 methodological details see Fuertes et al. (2014).

313 An estimated range of annual contributions of coccoliths to total CaCO<sub>3</sub> export  
314 was calculated for the 2000 m trap record by multiplying the coccolith flux of each  
315 sampling interval by the maximum and minimum standard deviations of coccolith weight  
316 values measured on each sample. Then, the minimum and maximum estimates of  
317 coccolith-CaCO<sub>3</sub> fluxes for each sampling interval (i.e. cup) were used to estimate the  
318 minimum and maximum annual contribution of coccoliths to total carbonate following  
319 the same procedure as for the annual coccolith fluxes.

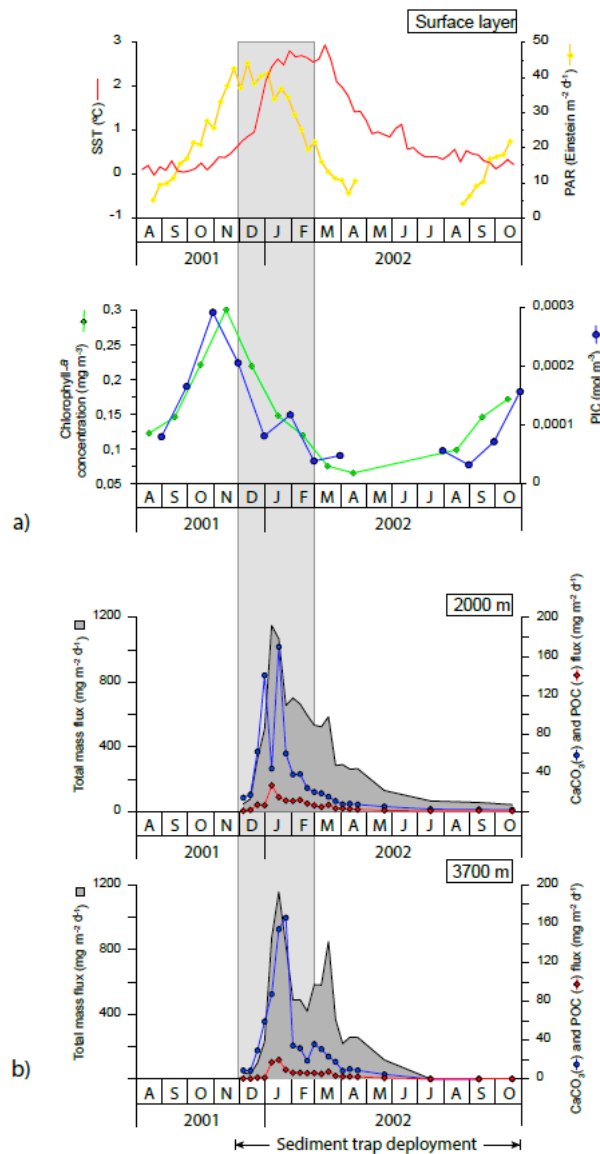
320

#### 321 **2.5 Satellite imagery, meteorological and oceanographic data**

322 Weekly mean SST for the 2001-2002 interval were obtained from the NOAA  
323 Optimum Interpolation SST Analysis database (Reynolds et al., 2002). Seasonal SST  
324 variation range was low, with maximum SSTs of 2.94 °C observed during March 2002  
325 and minimum of 0.12 °C, in early October 2002. SST variations mirrored changes in the  
326 vertical structure of the water column temperature profile (Fig. 4) that displayed vertical  
327 homogeneity of the water column in autumn and winter and a seasonal thermocline during  
328 the austral summer (Fig. 2b).

329 Sea surface salinity (SSS) climatology for the study site was obtained from the NOAA  
330 World Ocean Atlas 2005 (Antonov et al., 2006). SSS exhibited very low seasonal  
331 variability with values ranging between 33.7 and 33.9 psu.

332         Photosynthetically Active Radiation (PAR), monthly chlorophyll-*a* concentration  
333 and Particulate Inorganic Carbon (PIC) concentration estimates were obtained from  
334 NASA's Giovanni program (Acker and Leptoukh, 2007) (Fig. 4) for the region: 130°E,  
335 62.5°S, 150°E, 59.5°S. Chlorophyll-*a* concentration was low throughout the year (ranging  
336 from 0.07 to 0.30 mg m<sup>-3</sup>) and in line with previous observations in the study region (Trull  
337 et al., 2001b). Algal biomass responded rapidly to the solar radiation increase in  
338 September 2001 and reached its highest levels in November 2001 (Fig. 4). Chlorophyll-  
339 *a* concentration declined throughout the summer, reaching negligible values in autumn  
340 and winter (i.e. from March to August 2002). Satellite-derived PIC concentration  
341 exhibited a clear seasonal pattern similar to that of the chlorophyll-*a* with peak  
342 concentrations in November (up to 0.003 mol m<sup>-3</sup>) and values below detection limit in  
343 winter (Fig. 4).



344

345 **Figure 4:** (a) Satellite-derived SST (°C), PAR (Einstein m<sup>-2</sup> d<sup>-1</sup>), chlorophyll-*a*  
 346 concentration (mg m<sup>-3</sup>) and PIC concentration (mol m<sup>-3</sup>) for the period November 2001  
 347 to September 2002. It is important to note that satellite PIC concentration estimates have  
 348 been reported to be biased for high latitudes systems of the Southern Ocean where the  
 349 satellite algorithm is thought to produce overestimates (Balch et al., 2016; Trull et al.,  
 350 2017). Therefore PIC data presented here should be viewed with caution. (b) Temporal  
 351 variability of the total mass, CaCO<sub>3</sub> and POC the < 1mm fraction at 2000 and 3700 m  
 352 water depth from November 2001 through to November 2002 at the 61°S site (Rigual-  
 353 Hernández et al., 2015a). Grey strips represent summer.

354

### 355 3. Results

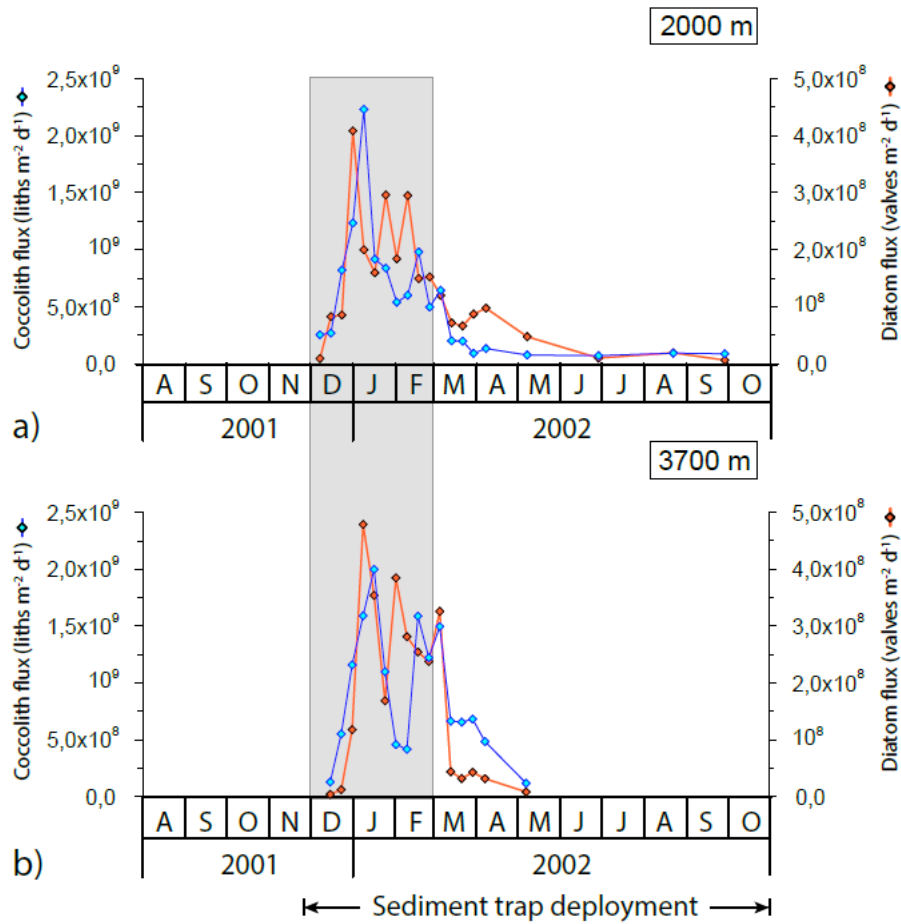
356

### 357 **3.1 Seasonal dynamics of coccolith export fluxes**

358 Coccolith fluxes showed a pronounced seasonal pattern at both sediment trap  
359 depths, roughly following the chlorophyll-*a* dynamics in the surface layer with maximum  
360 fluxes during the austral summer and minima during winter (Fig. 4 and 5). The summer  
361 coccolith flux exhibited a bimodal distribution with a major peak registered in early  
362 January ( $2.2 \times 10^9$  coccoliths  $\text{m}^{-2} \text{d}^{-1}$  at 2000 m) and a secondary maximum recorded in  
363 mid-February ( $9.8 \times 10^8$  coccoliths  $\text{m}^{-2} \text{d}^{-1}$ ). Coccolith flux was low in autumn and winter  
364 (down to  $\sim 7 \times 10^7$  coccoliths  $\text{m}^{-2} \text{d}^{-1}$ ). Coccolith fluxes in the deeper trap (3700 m)  
365 followed a similar pattern to that in the 2000 m trap with a delay of about one sampling  
366 interval.

367 The fluxes of all biogeochemical components were closely correlated (Table 2 in  
368 Rigual-Hernández et al., 2015a). Coccolith fluxes at both traps were broadly in line with  
369 biogenic particle fluxes estimated by Rigual-Hernández et al. (2015a) showing strongest  
370 correlations with biogenic silica ( $R^2 = 0.74$  at 2000 m and  $R^2 = 0.71$  at 3700 m), followed  
371 by PIC ( $R^2 = 0.62$  at 2000 m and  $R^2 = 0.47$  at 3700 m) and POC ( $R^2 = 0.56$  at 2000 m  
372 and  $R^2 = 0.41$  at 3700 m).

373 Coccolithophore sinking assemblages captured by the traps were nearly  
374 monospecific, with an overwhelming dominance of *E. huxleyi* that represented >99% of  
375 the annual coccolith sinking assemblage at both trap depths. Background concentrations  
376 of *Calcidiscus leptoporus* (*sensu lato*), *Gephyrocapsa* spp. and *Helicosphaera* spp. were  
377 also registered, together representing 0.6% and 0.3% of the coccolith assemblage at 2000  
378 and 3700 m, respectively, of the total annual coccolith fluxes (Table 1). The seasonal  
379 changes in the coccolithophore species flux and relative abundance can be found in  
380 Supplementary Figure 1. The seasonal pattern of *C. leptoporus* and *Gephyrocapsa* spp.  
381 followed that of *E. huxleyi* with peak values during the summer and minima during  
382 winter. The numbers of coccospheres found in the samples were negligible in both  
383 sediment trap records.



384

385 **Figure 5:** Seasonal variation of total coccolith and diatom valve flux at the 2000 and 3700  
 386 m sediment traps at the 61°S site. Grey strips represent summer.

387

### 388 3.2 SEM analyses

389 *Emiliania huxleyi* coccoliths correspond to morphotype B/C, having proximal  
 390 shields slightly wider than the distal ones and with a central area usually filled by several  
 391 (usually 5 to 11) flat, wide and thin tile-like elements (see Plate 1, image a). Distal shields  
 392 of several are partially missing, most likely due to the slender and delicate structure of  
 393 the laths. Distal shield measures ranged between 2 to 4.35  $\mu\text{m}$  in the samples recovered  
 394 from the 2000 m sediment trap. The coccoliths captured by the traps were clearly different  
 395 than those of morphotype A which is the other morphotype that has been reported in the  
 396 Australian sector of the Southern Ocean (Cubillos et al. 2007). Morphotype A has a  
 397 central area composed of curved elements (Young et al., 2003) and its distal shield  
 398 elements are more robust than those of B/C (Young et al., 2003). Since the size of the  
 399 coccoliths has been reported to vary significantly on the same coccosphere, coccolith size

400 was not used as a discriminatory feature to differentiate between morphotypes following  
401 Cubillos et al. (2007).

402 It is conspicuous that most of the coccoliths display a morphology which is  
403 compatible with a secondary recrystallisation. Small spherules like recrystallisations are  
404 present on these coccoliths, especially on the laths (Plate 1, images c-f). However, some  
405 coccoliths, mostly from cup 10 (February) have no spherules covering them (Plate 1,  
406 images a and b). Aside from this sample, no relationship between the morphology of the  
407 coccoliths and collection time was found. These coccoliths present very thin slender laths  
408 (usually from 20 to 26) and wider central areas than the coccoliths having spherules.

409

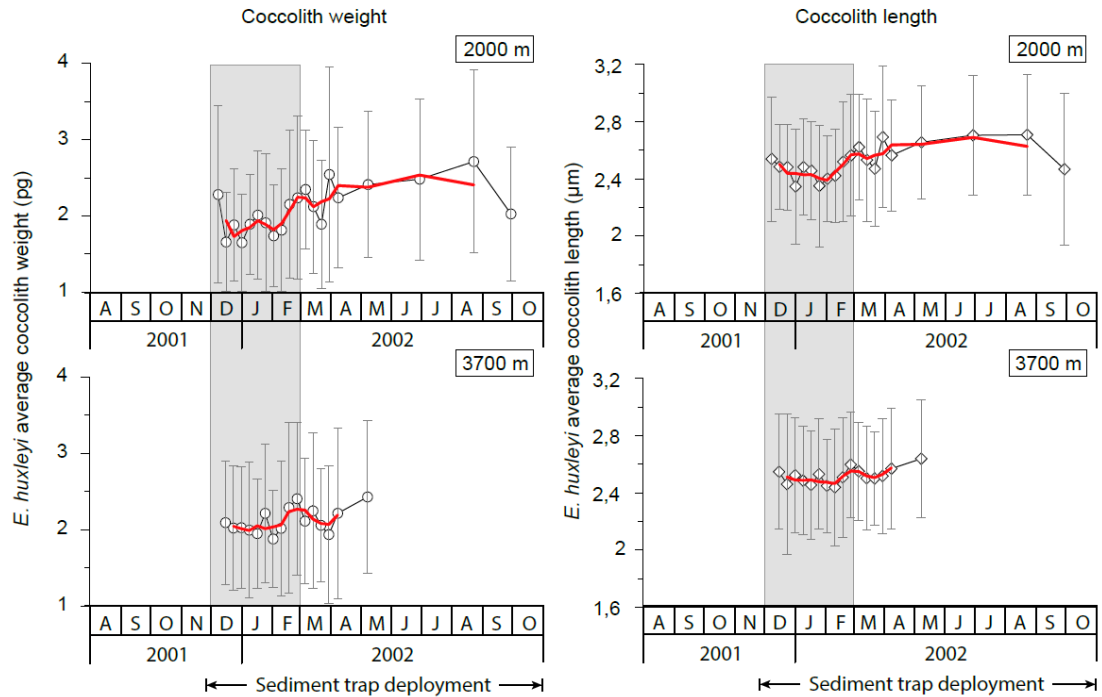
### 410 **3.3 Coccolith weight and length changes**

411 Average coccolith weight at both sediment trap depths exhibited a clear seasonal  
412 pattern with high values ( $2.28 \pm 1.16$  and  $2.09 \pm 0.80$  pg/coccolith at 2000 m and 3700  
413 m, respectively) at the onset of the coccolithophore productive period in early spring,  
414 followed by a pronounced decrease (down to  $1.65 \pm 0.63$  and  $1.88 \pm 0.63$  pg at 2000 m  
415 and 3700 m, respectively) in approximately January – early February. Average coccolith  
416 weight followed a gradual increasing trend from approximately mid-February into winter,  
417 reaching values up to  $2.71 \pm 1.20$  pg in August 2002 at 2000 m and up to  $2.43 \pm 1.00$  in  
418 May at 3700 m, respectively. Average annual coccolith weight was  $2.11 \pm 0.96$  and  $2.13$   
419  $\pm 0.91$  pg at 2000 and 3700 m, respectively. The annual amplitude of the mean coccolith  
420 weight was approximately 1 pg at 2000 m and 0.5 pg at 3700 m. The lower annual  
421 amplitude exhibited by the coccolith assemblages captured at the 3700 m trap is attributed  
422 to the lower sampling duration at that depth over the winter season.

423 Mean coccolith length was greatest in early spring 2001 ( $2.54 \pm 0.44$  and  $2.55 \pm$   
424  $0.40$   $\mu\text{m}$  at 2000 and 3700 m, respectively), followed by a decrease in early summer  
425 (down to  $2.35 \pm 0.43$  and  $2.44 \pm 0.41$   $\mu\text{m}$  at 2000 and 3700 m, respectively) (Fig. 6). From  
426 late February coccolith length increased again reaching the highest values of the record  
427 in winter 2002 (up to  $2.71 \pm 0.42$  and  $2.64 \pm 0.41$   $\mu\text{m}$  at 2000 and 3700 m, respectively).

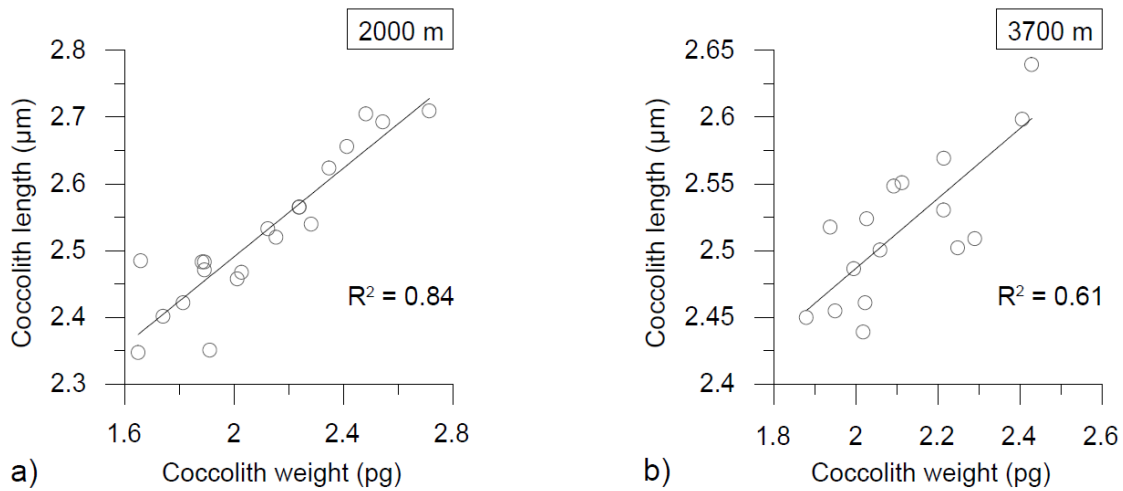
428 Seasonal variations of coccolith length and weight exhibited a strong correlation  
429 at both depths ( $R^2 = 0.84$ ,  $n = 20$  at 2000 m;  $R^2 = 0.61$ ,  $n = 16$  at 3700m), indicating a  
430 clear, dependable relationship between the two variables (Fig. 7).

431



432

433 **Figure 6:** Mean and standard deviation of coccolith weight and length over the sediment  
 434 trap deployment period at 2000 m and 3700 m at the 61°S site. The red solid line  
 435 represents a 3-point running average. Grey strips represent summer.



436

437 **Figure 7:** Regression plots between *E. huxleyi* coccolith mass (pg) and length (µm) at the  
 438 2000 m (a) and 3700 m (b) sediment traps.

439 **4. Discussion**

440 **4.1 Origin, magnitude and composition of the coccolithophores**

441 Since there is a current debate about the potential expansion of *E. huxleyi*  
 442 populations south of the PF during recent decades (Cubillos et al., 2007; Saavedra-

443 Pellitero et al., 2014; Winter et al., 2014; Malinverno et al., 2015; Patil et al., 2017), it is  
444 important to evaluate the likely origins of the sinking coccolith assemblages collected at  
445 station 61°S. This assessment is particularly needed in the case of deep-moored,  
446 sediment-trap experiments because the source area of the particles collected by the traps  
447 can be as wide as hundreds of square kilometres (Buesseler et al., 2007).

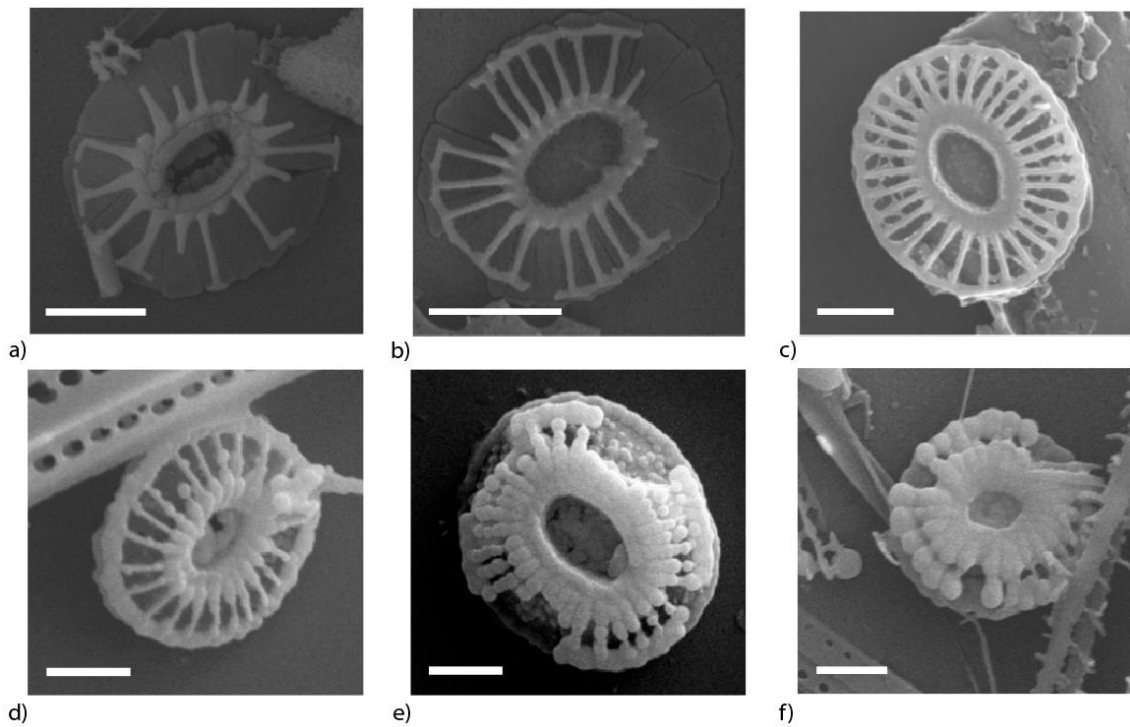
448 Several lines of evidence strongly suggest that the coccolithophore fluxes  
449 registered by the traps were produced in waters of the Antarctic Zone. Firstly, the mooring  
450 was deployed in a quiescent area of the AZ-S (Trull et al., 2001b), between the stronger  
451 flows associated with the southern branch of the PF and the SACCF (Fig. 1). The  
452 relatively weak currents around the sediment trap location greatly reduce the area of likely  
453 origins of the particles intercepted by the traps, i.e. the statistical funnel (Siegel and  
454 Deuser, 1997; Siegel et al., 2008). Moreover, the large magnitude of the coccolith export  
455 fluxes at both depths, plus the long duration of the period of enhanced coccolith flux  
456 (about 3 months), rule out the likelihood of a transient lateral transport event (e.g.,  
457 transport by mesoscale eddies) of a coccolithophore bloom produced in more northerly  
458 latitudes. Lastly, the composition of the biogeochemical fluxes and diatom assemblages  
459 collected by the traps are characteristic of AZ waters (Rigual-Hernández et al., 2015a),  
460 further supporting the idea that the coccolithophores captured by the traps were produced  
461 close to the site. All this clearly indicates that in 2001 *E. huxleyi* was an established  
462 member of the phytoplankton communities of the Antarctic Zone to the south of  
463 Australia.

464 The annual coccolith export to the deep ocean at the 61°S site ( $1.03 \times 10^{11}$   
465 coccoliths  $\text{m}^{-2} \text{yr}^{-1}$ ) is one sixth that registered by Wilks et al. (2017) ( $6.5 \times 10^{11}$  coccolith  
466  $\text{m}^{-2} \text{yr}^{-1}$ ) in the SAZ waters (station 47°S; Fig. 1) north of the study site. The lower  
467 abundance of coccolithophores at the sampling site is most likely due to the negative  
468 effects of low temperature and low light levels on coccolithophore growth (Paasche,  
469 2002; Boyd et al., 2010), but important also is the competitive advantage of diatoms over  
470 coccolithophores in the silicate-rich waters of the AZ-S. The lower coccolithophore  
471 production in the AZ-S is also reflected in the lower carbonate export at this site, i.e. 6 g  
472  $\text{m}^{-2} \text{y}^{-1}$  versus 10-13 g  $\text{m}^{-2} \text{y}^{-1}$  at the 47°S site (Rigual-Hernández et al., 2015b; Wilks et  
473 al., 2017). The non-proportional latitudinal change in coccolith and carbonate fluxes (i.e.  
474 sixfold versus twofold changes, respectively) is most likely due to variations in the  
475 contribution of heterotrophic calcifiers (i.e. foraminifers and pteropods) to total carbonate  
476 export. There are also differences in the carbonate content per coccolith of the

477 coccolithophore species and the morphotypes of *E. huxleyi* dwelling in each zonal system.  
478 Indeed, mean coccolith weight can vary up to two orders of magnitude between small  
479 species such as *E. huxleyi* (2-3.5 pg) and large and heavily calcified taxa such as  
480 *Coccolithus pelagicus* (~150 pg) (Giraudeau and Beaufort, 2007). Intraspecific size  
481 variability is also common in most coccolithophore species, mainly due to growth  
482 variations driven by different environmental factors and by genotypic variability (e.g.  
483 Knappertsbusch et al., 1997; Poulton et al., 2011).

484         Based on the significant genetic variability found between Southern Ocean  
485 populations of morphotypes A and B/C, Cook et al. (2011) classified these morphotypes  
486 as *E. huxleyi* var. *huxleyi* and *E. huxleyi* var. *aurorae*, respectively. Since only  
487 morphotype B/C had been reported at and south of the Antarctic Polar Front, Cook et al.  
488 (2013) concluded that the rapid drop in water temperature occurring at the Antarctic Polar  
489 Front may act as an open-ocean barrier to gene flow between these the two Southern  
490 Ocean *E. huxleyi* morphotypes/varieties. The nearly monospecific coccolith assemblages  
491 of *E. huxleyi* morphotype B/C collected by the 61°S site traps (Plate 1) are consistent with  
492 those studies and supports the idea that the physiological differences in light-harvesting  
493 pigments of morphotype B/C compared to other *E. huxleyi* varieties (Cook et al., 2011)  
494 may represent a critical ecological advantage in the cold and low-light waters of the AZ-  
495 S south of Australia.

496



498

499 **Plate 1:** SEM photos showcasing the different morphologies of *Emiliana huxleyi*  
 500 morphotype B/C coccoliths found in the sediment traps of the 61°S site. Scale bars =1  
 501  $\mu\text{m}$ .

502

#### 503 **4.2 Seasonal dynamics of the calcareous and siliceous phytoplankton fluxes**

504 The eight-day sampling resolution during spring and summer enabled us to  
 505 monitor the detailed temporal dynamics of phytoplankton fluxes at the 61°S site.  
 506 Comparison of satellite-derived PIC and chlorophyll-*a* concentrations for the study region  
 507 with coccolith fluxes registered by the sediment trap suggests a time lag of about two  
 508 months between their surface maxima and peak coccolith fluxes registered by the  
 509 shallower trap (Fig. 4). Therefore, the growth phase of the *E. huxleyi* bloom probably  
 510 took place between October and December 2001, a period characterised by very low SSTs  
 511 (0.1-0.9 °C). It was before development of any significant stratification in the upper water  
 512 column (Fig. 2b and 4a). These observations indicate that the very cold temperatures (near  
 513 0°C) and strong mixing of the water column in the Antarctic waters during spring are not  
 514 an impediment for the development of an *E. huxleyi* bloom. The very low *C. leptoporus*  
 515 and *Gephyrocapsa* spp. fluxes throughout the annual cycle suggest that the environmental  
 516 conditions of the AZ-S must represent an ecological limit of these species. Peak fluxes of

517 *C. leptoporus* and *Gephyrocapsa* spp at both sediment traps coincide with those of *E.*  
518 *huxleyi* indicating that the summer solar irradiance increase is the main factor stimulating  
519 coccolithophore growth irrespectively of the species.

520         The onset of seasonal increase in coccolithophore arrivals in the traps occurred at  
521 the same time as that of diatoms, suggesting a rapid response of both phytoplankton  
522 groups to enhanced light levels. Although both coccolith and diatom fluxes exhibited a  
523 pronounced and nearly parallel increase throughout December (Fig. 5), coccolith fluxes  
524 peaked one week later than those of diatoms. A similar succession was observed in late  
525 summer, when coccoliths displayed a secondary flux maximum, one sampling interval  
526 later (8 days) than that of diatoms (Fig. 5). These observations agree with the bloom-  
527 dynamics scheme proposed by Barber and Hiscock (2006) (the so-called coexistence  
528 theory), in that neither phytoplankton group seems to outcompete the other during the  
529 development of the bloom. Interestingly, diatoms seem to decline earlier than  
530 coccolithophores, a feature often (but not always) observed in other parts of the world  
531 ocean (e.g. Margalef, 1978; Holligan et al., 1983; Lochte et al., 1993; Sieracki et al., 1993;  
532 Thunell et al., 1996; Balch, 2004). Indeed, a recent study of the phenological  
533 characteristics of coccolithophore blooms by Hopkins et al. (2015) concluded that they  
534 often follow those of diatoms in many regions, the sequencing driven by increasing  
535 stabilization and/or nutrient depletion (mainly silicate and/or iron, and possibly also  
536 favoured by associated increase of carbonate saturation; Merico et al, 2004) of the surface  
537 layer. The slightly different seasonal pattern observed at both sampling depths (Fig. 5) is  
538 mainly attributed to the fact that the area of the ocean from which the particles have been  
539 produced increases with depth (Siegel and Deuser, 1997).

540         Lack of nutrient and mixed-layer-depth measurements during the sediment trap  
541 deployment precludes us from establishing robust links between changes in physical and  
542 chemical parameters in the upper water column and the observed phytoplankton  
543 succession. Nonetheless, some shipboard observations of mixed-layer properties from  
544 years previous to the sediment trap deployment (Fig. 2; Trull et al., 2001b) can provide  
545 some insight about the mechanisms driving the phytoplankton succession. Macronutrient  
546 measurements indicate that, although considerable nutrient draw-down often occurs by  
547 mid-summer, the AZ-S waters never reach potentially limiting concentrations (i.e. below  
548 10  $\mu\text{M}$ ) of silicate, nitrate or phosphate (Fig. 2a; Trull et al., 2001b). Thus, macronutrient  
549 limitation was not a likely driver of the observed phytoplankton succession at the 61°S  
550 site traps. Iron levels in the AZ-S, on the other hand, are low year-round (0.1-0.2 nM;

551 Boyd et al., 2000b; Sohrin et al., 2000) and exhibit clear seasonality in the AZ (Tagliabue  
552 et al., 2014). So, iron availability does represent a potential driver for the observed  
553 phytoplankton succession. Indeed, laboratory experiments have shown that *E. huxleyi* has  
554 lower minimum iron requirements for growth than oceanic diatoms (Brand et al., 1983;  
555 Muggli and Harrison, 1997). This physiology likely provides an ecological advantage  
556 over diatoms in the later stages of the spring-summer bloom, when most iron has been  
557 stripped from the mixed layer.

558 In regard to the mechanism underlying the second diatom-coccolith succession  
559 observed at both depths in February (Fig. 5), it is possible that a vertical mixing event –  
560 as frequently reported in the AZ (e.g. Brzezinski et al., 2001) – supplied waters rich in  
561 iron and macronutrients to the euphotic zone, resetting the phytoplankton succession.  
562 Alternatively, the part of the *E. huxleyi* populations accumulated at or just above the  
563 nutricline may have increased using the iron moved by diapycnal diffusion through the  
564 pycnocline (Tagliabue et al., 2014). Their deposition in February could have been  
565 triggered by a drop of the light levels (Fig. 4). This second hypothesis is also consistent  
566 with the following observations: (1) the presence of a sub-surface chlorophyll-*a*  
567 maximum in the study region during spring and summer (Parslow et al., 2001; Trull et  
568 al., 2001b); (2) reports of high *E. huxleyi* cell accumulations associated with the nutricline  
569 in other settings of the world ocean (Beaufort et al., 2008; Henderiks et al., 2012) and (3)  
570 peak annual sedimentation in late February of the diatom *Thalassiothrix antarctica*  
571 (Rigual-Hernández et al., 2015a), a typical component of the “shade flora” (Kemp et al.,  
572 2000; Quéguiner, 2013). Further sampling and taxonomic analysis of the vertical  
573 distributions of phytoplankton in the AZ-S south of Australia are required to assess these  
574 hypotheses.

575

#### 576 **4.3 Seasonal variability in coccolith calcification**

577 Two main factors have been proposed as driving seasonal changes in coccolith  
578 weights of *E. huxleyi*: a seasonal shift in the dominant morphotypes/ecotypes — each  
579 with a different degree of calcification (Poulton et al., 2011) — and the physiological  
580 response of a given morphotype to the seasonal variation of environmental parameters  
581 (e.g. Smith et al., 2012; Meier et al., 2014). SEM analysis of the sediment trap samples  
582 revealed that only morphotype B/C, *sensu* Young et al. (2003), thrives in the AZ-S waters  
583 south of Tasmania. That is consistent with a report by Cubillos et al. (2007) of dominance  
584 of B/C south of 50°S. Therefore, a seasonal shift in the dominant morphotype can be ruled

585 out in respect to changing coccolith weight. The observed decrease in coccolith weight  
586 could have been caused by a change in coccolith calcification or reduction in coccolith  
587 dimensions. Young and Ziveri (2000) showed that coccolith weight is approximately  
588 linearly correlated to the cube of coccolith length. Applying that, the decrease in length  
589 by 7.5% (a reduction to 92.5%) observed from the pre-bloom to the summer bloom in the  
590 2000 m traps (i.e. difference in minimum coccolith lengths in cups 5 and 8) corresponds  
591 to a coccolith weight loss of 21% ( $0.925^3 \approx 0.79$ ). That is similar to the observed weight  
592 reduction in the 2000 m trap between the pre-bloom and summer bloom coccolith  
593 assemblages (16.2 - 27.6%, respectively Fig. 6). When the linear correlation between  
594 coccolith length and weight proposed by Young and Ziveri (2000) is also applied to the  
595 3700 m trap coccoliths, the predicted reduction of coccolith weight between the pre-  
596 bloom and bloom assemblages is 12%. That is again very similar to the reduction in  
597 coccolith weight observed in the *E. huxleyi* coccoliths intercepted by the 3700 trap (10%).  
598 It is strongly suggested that the seasonal changes in coccolith weight at the 61°S site were  
599 mainly driven by changes in coccolith length and were not due to significant changes in  
600 their degrees of calcification.

601 Laboratory, mesocosm and field studies have shown that multiple environmental  
602 factors including light, temperature, salinity, seawater carbonate chemistry,  
603 macronutrient concentrations and iron availability affect coccolith formation by *E.*  
604 *huxleyi* cells (e.g. Paasche, 2002; Zondervan, 2007; Langer and Benner, 2009; Feng et  
605 al., 2017). We examine each of these factors in turn, but note that all exhibit correlated  
606 seasonal cycles and thus identification of a single driver is particularly difficult.

607 Since calcification in *E. huxleyi* is a light-dependent process (Paasche, 1999,  
608 2002), the observed decrease in coccolith weight during summer in both traps is not an  
609 obvious response to increasing light in summer. However, Paasche and Brubak (1994)  
610 observed that calcification is less strongly curtailed than photosynthesis under low light  
611 conditions, so that perhaps high calcification relative to growth in winter could lead to  
612 heavier coccolith weights in that part of the seasonal cycle. Interestingly, this would  
613 contrast with a recent synthesis of results for another coccolithophore, *Gephyrocapsa*  
614 *oceanica*, in which optimal light for calcification was found to be slightly higher than for  
615 photosynthesis or growth (Gafar et al., 2018), emphasizing that the sensitivities of these  
616 processes may be organism and possibly even strain specific. Smith et al. (2010)  
617 previously documented a reduction in coccolith calcification of *E. huxleyi* coccospheres  
618 during the summer months in the Bay of Biscay, but advised caution in associating this

619 with light intensity because calcification rates may not necessarily covary with the  
620 amount of calcite content per coccolith. Therefore, the possible effect of light intensity  
621 on coccolith weight in our traps is plausible but not demonstrable with our current data.

622 In terms of temperature effects, Saruwatari et al. (2016) described a decrease in  
623 coccolith size with increasing temperature cultivating *E. huxleyi* strains (morphotype B/C,  
624 strains MR57N and MR70N) from the Bering and Chukchi Seas. However, comparison  
625 of our results with those of Saruwatari et al. (2016) should be done with great caution due  
626 to two reasons. Firstly, the *E. huxleyi* coccolithophores living in the Arctic seas most  
627 likely correspond to a different ecotype than those dwelling in the AZ waters, and  
628 therefore they may potentially exhibit different physiological responses to water  
629 temperature changes. Secondly, the SST range in our study site was remarkably lower (0  
630 - 3°C) than that used by Saruwatari et al. (2016) in their cultures (5 - 20°C). These  
631 limitations make drawing inferences from Saruwatari et al. (2016) difficult. Feng et al.  
632 (2017), on the other hand, showed that optimal temperature for calcification of *E. huxleyi*  
633 cells retrieved in the Southern Ocean (morphotype A, strain NIWA1108) was ~20°C,  
634 while temperatures below 10°C resulted in a dramatic reduction of calcification rates and  
635 severe malformations of coccoliths, such as incomplete distal shield elements. Although  
636 *E. huxleyi* morphotype B/C found at the 61°S site likely represents an ecotype more  
637 tolerant to low temperatures than morphotype A (Cubillos et al., 2007; Cook et al., 2013),  
638 the frequent variations in the structure of the coccoliths (e.g. incomplete distal shield  
639 elements; Plate 1) captured by the traps suggest some degree of low-temperature stress.  
640 Despite the important role of temperature in coccolithophore growth (Paasche, 2002),  
641 enhanced summer SSTs may lead to an increase in coccolith weight, a response opposite  
642 to that observed at both traps. Therefore, it is unlikely that seasonal SST variations at the  
643 61°S are behind the observed variability in coccolithophore weight.

644 For salinity, Bollmann and Herrle (2007) identified a close relationship between  
645 changes in SSS (gradient from 33 to 38) and the length of *E. huxleyi* coccoliths using a  
646 global compilation of core top and plankton samples. However, based on the almost  
647 negligible annual variability in SSS (values ranging between 33.7 to 33.9 psu) in the study  
648 region, salinity most likely did not play a significant role on the observed seasonal  
649 variability in coccolith morphology observed in our traps.

650 In regard to the possible impact of macronutrient concentrations on coccolith  
651 weight, both nitrate and phosphate are known to have a pronounced effect on coccolith

652 calcite content and morphology (Zondervan, 2007). However, as mentioned previously,  
653 none of these macronutrients reach limiting concentrations throughout the annual cycle  
654 in the AZ-S (Fig. 2; Trull et al., 2001b). and therefore, their influence in the calcification  
655 of coccolithophores is likely to be low or negligible.

656 Seawater carbonate chemistry is a known driver of calcification in  
657 coccolithophores, with decreased growth and calcification attributable to both lower pH  
658 and carbonate saturation state, e.g. as summarized in a recent model capable of  
659 reproducing a wide range of experimental observations (Bach et al., 2015). But the  
660 seasonal cycle in carbonate saturation and pH in Antarctic waters is driven by net  
661 community production so that both are higher in summer (Shadwick et al., 2013; 2015a;  
662 2015b) and thus would be more likely to favour higher shell weights in opposition to the  
663 observations.

664 On the other hand, low iron levels have been reported to have a pronounced  
665 negative effect on  $\text{CaCO}_3$  production by *E. huxleyi* cells (Schulz et al., 2004), so it  
666 represents a candidate driver of seasonal changes in coccolith weight. During winter, deep  
667 water mixing re-stocks the mixed layer with iron (Tagliabue et al., 2014). As soon as light  
668 levels become sufficient for photosynthesis in early spring, phytoplankton rapidly  
669 develops under non-limiting concentrations of macro- and micronutrients. These  
670 favourable conditions for coccolithophore growth could explain the heavier and larger  
671 coccoliths registered in early December (Fig. 6). As the phytoplankton bloom develops,  
672 the dissolved iron stock is rapidly depleted in the photic zone possibly resulting in a size  
673 and weight reduction of coccoliths of the already substantial *E. huxleyi* populations. From  
674 late summer throughout autumn, some recycling of iron in the upper water column by  
675 increasing summer populations of zooplankton feeding on the bloom (Tagliabue et al.,  
676 2014), coupled with increasing light levels and the continued shallowing of the mixed  
677 layer, would allow coccolithophores to produce again longer and heavier coccoliths (Fig.  
678 6).

679 Changes in light intensity in the mixed layer and/or iron-limitation, therefore,  
680 represent the most likely environmental driving factors for the seasonal variability in  
681 coccolith weight and length of *E. huxleyi* assemblages at the 61°S site. However, we note  
682 again that the lack of fitness response experiments on Southern Ocean strains of *E. huxleyi*  
683 morphotype B/C to varying environmental conditions and lack of *in situ* measurements  
684 of chemical and physical parameters of the water column, mean that control of coccolith

685 weight by light and/or iron availability in the AZ-S remain as an hypothesis needing  
686 validation by future studies.

687

#### 688 **4.4 Effects of calcite dissolution on the sinking coccolith assemblages**

689 The similar average annual coccolith weight registered at both traps indicates that  
690 negligible coccolith dissolution occurs at meso- and bathypelagic depths in the AZ-S  
691 south of Australia. That is despite the fact that coccolith sinking assemblages captured by  
692 the deeper trap were exposed to potentially intense dissolution after crossing the CSH  
693 (located at 3000 m in the study region; Fig. 2). The similar coccolith values observed at  
694 both depths can be attributed to the formation of algal and faecal aggregates in the mixed  
695 layer that include fine mineral particles (Passow and De La Rocha, 2006) and provide  
696 protection against dissolution. They also facilitate rapid transport of the coccoliths down  
697 through the water column. The aggregate-formation hypothesis is supported by the  
698 findings of Closset et al. (2015) who estimated that sinking rates at the 61°S site were, at  
699 least 213 m d<sup>-1</sup> during the productive period, a value consistent with the sinking rates of  
700 algal and/or faecal aggregates (Turner, 2002, 2015).

701 Despite not finding increased dissolution with water depth between 2000 and 3700  
702 m, it is possible that coccoliths experienced some carbonate dissolution before reaching  
703 the traps. Milliman et al. (1999) suggested that the same biological processes that  
704 facilitate aggregate formation and flocculation, such as ingestion, digestion and egestion  
705 by grazers, may be responsible for significant carbonate dissolution at epipelagic depths  
706 (i.e. depths shallower than 800-1000 m. Indeed, the negligible amounts of coccospheres  
707 found in both traps, together with the high sinking velocities, suggest that grazing could  
708 have been an important influence on export. That is supported by findings of Ebersbach  
709 et al. (2011) in the PFZ north of our study location. They documented that an important  
710 fraction of the particles sinks from the mixed layer as faecal aggregates. On the other  
711 hand, the small spherules often observed on the coccoliths captured by the traps suggest  
712 some degree of coccolith dissolution followed by remineralisation. We speculate that  
713 some of the coccoliths captured by the traps could have experience partial dissolution in  
714 the upper water column leading to the exposure of their organic coccolith scaffold (Gal  
715 et al., 2016; Lee et al., 2016) to the environment. It is possible that salts dissolved in the  
716 water column subsequently precipitated over this scaffold structures resulting in the  
717 formation of the recrystallised structures observed in some coccoliths (Plate I, e-g).  
718 However, the available data are insufficient to evaluate the impact of carbonate

719 dissolution in the upper water column and processes leading to secondary recrystallisation  
720 in the coccoliths.

721

#### 722 **4.5 Calcium carbonate content of *Emiliana huxleyi* coccoliths**

723 A broad range of calcite contents for *E. huxleyi* coccoliths (1.4 - 7.0 pg) has been  
724 proposed in the literature (e.g. Young and Ziveri, 2000; Beaufort, 2005; Holligan et al.,  
725 2010; Poulton et al., 2011). The differences in these estimates are most likely due to  
726 variability in the amount of coccolith calcite between morphotypes and to the varied  
727 methodological biases associated with the three main approaches for estimating coccolith  
728 mass: morphometrics, regression and birefringence. Since *E. huxleyi* morphotype B/C is  
729 considered to be geographically restricted to the Southern Ocean (Cubillos et al., 2007;  
730 Cook et al., 2013) we limit the comparison of our results to studies conducted only in the  
731 Southern Ocean reporting this morphotype.

732 Average annual coccolith quotas at both trap depths at the 61°S site ( $2.11 \pm 0.96$   
733 and  $2.13 \pm 0.91$  pg per coccolith at 2000 m and 3700 m, respectively) are almost identical  
734 to that estimated by Holligan et al. (2010) ( $2.20 \pm 0.60$  pg ; morphotype B/C) in the Scotia  
735 Sea using a regression line between the number of coccoliths against PIC. Moreover, our  
736 estimates are slightly higher, but with a considerable overlap in the ranges of coccolith  
737 weight, than those estimated by Poulton et al (2011) for the *E. huxleyi* morphotype B/C  
738 populations found in Patagonian shelf waters ( $1.40 \pm 0.6$  pg). The greater standard  
739 deviation of our data is most likely due to the time periods compared. While the average  
740 coccolith weight estimated for our traps reflects an integration of the annual variability in  
741 coccolith weight, the shipboard observations by Poulton et al. (2011) provide a snapshot  
742 of the summer coccolithophore populations, that likely exhibit lower coccolith size and,  
743 thus, variability.

744 Because our coccolith weight estimates are similar to those of Poulton et al. (2011)  
745 and Holligan et al. (2010), we can estimate the fractional contribution of coccolithophores  
746 to total carbonate production in the AZ-S south of Australia. Coccolithophores account  
747 for approximately 2-5% of the annual deep-ocean CaCO<sub>3</sub> fluxes at mesopelagic depths at  
748 the 61°S site. The contribution of coccolithophores to the annual CaCO<sub>3</sub> budget in the  
749 AZ-S south of Australia is similar to the estimate by Salter et al. (2014) for the  
750 macronutrient-rich, but iron deficient M6 site in the Indian sector of the AZ (12%) and  
751 remarkably lower than an estimate for the iron-fertilised station A3 over the central  
752 Kerguelen Plateau (85%; Rembauville et al., 2016). Due to the different methodologies

753 for estimating coccolithophore contributions to carbonate production, comparison of our  
754 results with these other studies should be treated with caution. While only whole  
755 coccoliths were counted for our calculation, therefore providing a conservative estimate,  
756 Salter et al. (2014) and Rembauville et al. (2016) estimated the weight of the < 20 µm  
757 fraction using inductively coupled plasma-atomic emission spectrometry. That approach  
758 often results in overestimates of the coccolith contribution to bulk carbonate content.  
759 There can be non-negligible contributions of non-coccolith fragments to the fine fraction  
760 (Giraudeau and Beaufort, 2007). Despite the biases associated with both methodologies,  
761 the general trend appears clear: the fractional contributions of coccolithophores to bulk  
762 carbonate export are lower in the iron-limited waters of the AZ compared to those in  
763 naturally iron-fertilised settings of the Southern Ocean. These findings underscore the  
764 secondary role of this phytoplankton group in the biological carbon pumps (both the in  
765 organic carbon and carbonate counter pumps) south of the PF where non-calcifying  
766 phytoplankton - mainly diatoms and *Phaeocystis* - largely control the biologically-  
767 mediated CO<sub>2</sub> exchange between the ocean and the atmosphere.

768

## 769 **Conclusions**

770 Analysis of the materials captured by two sediment traps deployed at the 61°S site  
771 allowed for the characterization and quantification of coccolith assemblages in Australian  
772 sector of the Antarctic Zone. The data presented here provide a baseline of the state of  
773 coccolithophore populations in this region against which future changes can be assessed.  
774 More specifically, our study has shown the following:

- 775 • Coccolithophores were a consistent member of the phytoplankton communities of the  
776 Antarctic Zone south of Australia in year 2001. Coccolithophore assemblages in this  
777 region are monospecific being composed almost entirely of *Emiliana huxleyi*  
778 morphotype B/C. This observation supports the hypothesis that the physiological  
779 differences in light-harvesting pigments of morphotype B/C (or *E. huxleyi* var.  
780 *aurorae*), compared to other Southern Ocean *E. huxleyi* varieties (Cook et al., 2011),  
781 may represent an ecological advantage in the cold, low-light and iron-limited  
782 environment of the Antarctic Zone.
- 783 • The onset of the coccolithophore productive period took place at the same time as that  
784 of diatoms, indicating that neither phytoplankton group outcompetes the other during  
785 the development of the bloom. We speculate that the diatom-coccolithophore  
786 succession observed during the peak phase of the productive period could result from

787 the lower minimum iron requirements for growth of *E. huxleyi*, a feature that may  
788 confer a competitive advantage over diatoms.

789 • A decrease in coccolith weight and size during the summer months was observed at  
790 both sediment trap depths. After assessing the potential influence of several  
791 environmental parameters, changes in light intensity in the mixed layer and increasing  
792 iron limitation seem to be the most likely candidates to drive this change. These  
793 hypotheses, however, will need to be validated in future field and laboratory culture  
794 experiments with morphotype B/C.

795 • The similar weight of *E. huxleyi* coccolith assemblages captured by the 2000 and 3700  
796 m sediment traps indicates that negligible coccolith dissolution occurs during transit  
797 through meso- and bathypelagic depths in the study region. This is most likely due to  
798 a rapid transport of the coccoliths in algal and/or faecal aggregates.

799 • Coccolith weight values calculated for both sediment trap records using a  
800 birefringence-based approach were similar to previous estimates of *E. huxleyi*  
801 morphotype B/C in other Southern Ocean settings using regression and morphometric  
802 methods (Holligan et al., 2010; Poulton et al., 2011, respectively).

803 • Coccolithophore fluxes at the 61°S site account for only 2-5% of the annual deep-  
804 ocean CaCO<sub>3</sub> fluxes, suggesting that heterotrophic calcifiers must represent the main  
805 biogenic carbonate producer in the AZ-S south of Australia.

806

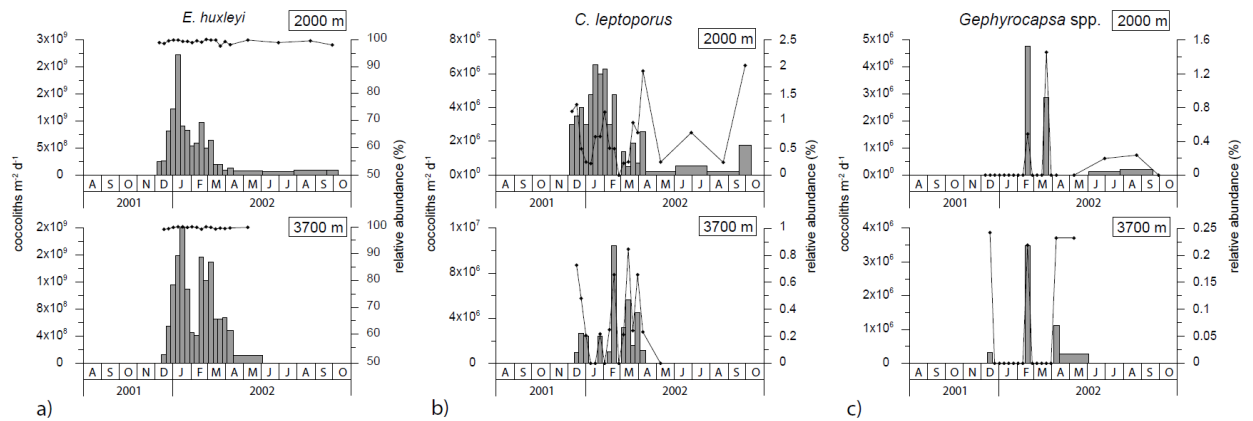
## 807 **Acknowledgments**

808 Sediment trap deployments and sample processing were carried out by ACE CRC staff  
809 (including Stephen Bray and Diana Davies) with support from the Australian  
810 Commonwealth Cooperative Research Centres Program and Australian Antarctic  
811 Division (via AAS Awards 1156 and 2256 to T. W. Trull). Subsampling for coccolith  
812 analysis was made possible by the Australian Government's Australian Antarctic Science  
813 Grant Program (project number 4078) and Macquarie University (Leanne K. Armand, A.  
814 Rigual-Hernández and T. W. Trull). Leanne K. Armand is acknowledged for her support  
815 in this study. We would like to express our sincere thanks to two anonymous reviewers  
816 and Emilio Marañón for valuable comments and remarks that greatly helped to improve  
817 the manuscript. This project has received funding from the European Union's Horizon  
818 2020 research and innovation programme under the Marie Skłodowska-Curie grant

819 agreement Number 748690 — SONAR-CO2 (A. Rigual-Hernández and J.A. Flores). We  
820 thank Charlie B. Miller for English corrections and comments on the manuscript.

821

## 822 Supplements



823

824 **Supplementary Figure 1:** Seasonal variation of flux and relative abundance of the main  
825 coccolithophore species captured by the 2000 and 3700 m trap: (a) *Emiliana huxleyi*, (b)  
826 *Calcidiscus leptoporus* and (c) *Gephyrocapsa* spp..

827

## 828 References

- 829 Acker, J. G., and Leptoukh, G.: Online Analysis Enhances Use of NASA Earth Science Data, Eos,  
830 Transactions. AGU, 88, 14-17, 2007.
- 831 Anderson, R. F., Ali, S., Bradtmiller, L. I., Nielsen, S. H. H., Fleisher, M. Q., Anderson, B. E., and  
832 Burckle, L. H.: Wind-Driven Upwelling in the Southern Ocean and the Deglacial Rise in  
833 Atmospheric CO<sub>2</sub>, Science, 323, 1443-1448, 10.1126/science.1167441, 2009.
- 834 Andersson, A. J., and Gledhill, D.: Ocean acidification and coral reefs: effects on breakdown,  
835 dissolution, and net ecosystem calcification, Annual Review of Marine Science, 5, 321-348,  
836 2013.
- 837 Antonov, J. I., Locarnini, R. A., Boyer, T. P., Mishonov, A. V., and Garcia, H. E.: World Ocean  
838 Atlas 2005, Volume 2: Salinity. S. Levitus, Ed. NOAA Atlas NESDIS 62,, U.S. Government  
839 Printing Office, Washington, D.C., 182 pp., 2006.
- 840 Archer, D., and Maier-Reimer, E.: Effect of deep-sea sedimentary calcite preservation on  
841 atmospheric CO<sub>2</sub> concentration, Nature, 367, 260-263, 1994.
- 842 Armstrong, R. A., Lee, C., Hedges, J. I., Honjo, S., and Wakeham, S. G.: A new, mechanistic  
843 model for organic carbon fluxes in the ocean based on the quantitative association of POC with  
844 ballast minerals, Deep Sea Research Part II: Topical Studies in Oceanography, 49, 219-236,  
845 [http://dx.doi.org/10.1016/S0967-0645\(01\)00101-1](http://dx.doi.org/10.1016/S0967-0645(01)00101-1), 2002.
- 846 Arrigo, K. R., Robinson, D. H., Worthen, D. L., Dunbar, R. B., DiTullio, G. R., VanWoert, M., and  
847 Lizotte, M. P.: Phytoplankton Community Structure and the Drawdown of Nutrients and CO<sub>2</sub> in  
848 the Southern Ocean, Science, 283, 365-367, 10.1126/science.283.5400.365, 1999.
- 849 Arrigo, K. R., DiTullio, G. R., Dunbar, R. B., Robinson, D. H., VanWoert, M., Worthen, D. L., and  
850 Lizotte, M. P.: Phytoplankton taxonomic variability in nutrient utilization and primary

851 production in the Ross Sea, *Journal of Geophysical Research: Oceans*, 105, 8827-8846,  
852 10.1029/1998JC000289, 2000.

853 Bach, L. T., Riebesell, U., Gutowska, M. A., Federwisch, L., and Schulz, K. G.: A unifying concept  
854 of coccolithophore sensitivity to changing carbonate chemistry embedded in an ecological  
855 framework, *Progress in Oceanography*, 135, 125-138,  
856 <https://doi.org/10.1016/j.pocean.2015.04.012>, 2015.

857 Balch, W. M.: Re-evaluation of the physiological ecology of coccolithophores, in:  
858 *Coccolithophores. From Molecular Processes to Global Impact.*, edited by: Thierstein, H. R.,  
859 and Young, J. R., Springer- Verlag, Berlin, 165–190, 2004.

860 Balch, W. M., Drapeau, D. T., Bowler, B. C., Lyczkowski, E., Booth, E. S., and Alley, D.: The  
861 contribution of coccolithophores to the optical and inorganic carbon budgets during the  
862 Southern Ocean Gas Exchange Experiment: New evidence in support of the “Great Calcite Belt”  
863 hypothesis, *Journal of Geophysical Research: Oceans*, 116, n/a-n/a, 10.1029/2011JC006941,  
864 2011.

865 Balch, W. M., Bates, N. R., Lam, P. J., Twining, B. S., Rosengard, S. Z., Bowler, B. C., Drapeau, D.  
866 T., Garley, R., Lubelczyk, L. C., Mitchell, C., and Rauschenberg, S.: Factors regulating the Great  
867 Calcite Belt in the Southern Ocean and its biogeochemical significance, *Global Biogeochemical  
868 Cycles*, 30, 1124-1144, 10.1002/2016GB005414, 2016.

869 Barber, R. T., and Hiscock, M. R.: A rising tide lifts all phytoplankton: Growth response of other  
870 phytoplankton taxa in diatom-dominated blooms, *Global Biogeochemical Cycles*, 20, n/a-n/a,  
871 10.1029/2006GB002726, 2006.

872 Barnett, T. P., Pierce, D. W., AchutaRao, K. M., Gleckler, P. J., Santer, B. D., Gregory, J. M., and  
873 Washington, W. M.: Penetration of Human-Induced Warming into the World's Oceans,  
874 *Science*, 309, 284-287, 10.1126/science.1112418, 2005.

875 Beaufort, L.: Weight estimates of coccoliths using the optical properties (birefringence) of  
876 calcite, *Micropaleontology*, 51, 289-297, 10.2113/gsmicropal.51.4.289, 2005.

877 Beaufort, L., Couapel, M., Buchet, N., Claustre, H., and Goyet, C.: Calcite production by  
878 coccolithophores in the south east Pacific Ocean, *Biogeosciences*, 5, 1101-1117, 2008.

879 Beaufort, L., Probert, I., de Garidel-Thoron, T., Bendif, E. M., Ruiz-Pino, D., Metzl, N., Goyet, C.,  
880 Buchet, N., Coupel, P., Grelaud, M., Rost, B., Rickaby, R. E. M., and de Vargas, C.: Sensitivity of  
881 coccolithophores to carbonate chemistry and ocean acidification, *Nature*, 476, 80-83,  
882 [http://www.nature.com/nature/journal/v476/n7358/abs/nature10295.html#supplementary-](http://www.nature.com/nature/journal/v476/n7358/abs/nature10295.html#supplementary-information)  
883 [information](http://www.nature.com/nature/journal/v476/n7358/abs/nature10295.html#supplementary-information), 2011.

884 Bollmann, J., and Herrle, J. O.: Morphological variation of *Emiliana huxleyi* and sea surface  
885 salinity, *Earth and Planetary Science Letters*, 255, 273-288,  
886 <https://doi.org/10.1016/j.epsl.2006.12.029>, 2007.

887 Bopp, L., Monfray, P., Aumont, O., Dufresne, J.-L., Le Treut, H., Madec, G., Terray, L., and Orr, J.  
888 C.: Potential impact of climate change on marine export production, *Global Biogeochemical  
889 Cycles*, 15, 81-99, 10.1029/1999GB001256, 2001.

890 Bostock, H. C., Hayward, B. W., Neil, H. L., Currie, K. I., and Dunbar, G. B.: Deep-water  
891 carbonate concentrations in the southwest Pacific, *Deep Sea Research Part I: Oceanographic  
892 Research Papers*, 58, 72-85, <http://dx.doi.org/10.1016/j.dsr.2010.11.010>, 2011.

893 Boyd, P., and Newton, P.: Evidence of the potential influence of planktonic community  
894 structure on the interannual variability of particulate organic carbon flux, *Deep Sea Research  
895 Part I: Oceanographic Research Papers*, 42, 619-639, [http://dx.doi.org/10.1016/0967-](http://dx.doi.org/10.1016/0967-0637(95)00017-Z)  
896 [0637\(95\)00017-Z](http://dx.doi.org/10.1016/0967-0637(95)00017-Z), 1995.

897 Boyd, P., Watson, A., Law, C., Abraham, E., Trull, T., Murdoch, R., Bakker, D., Bowie, A.,  
898 Buesseler, K., and Chang, H.: Phytoplankton bloom upon mesoscale iron fertilisation of polar  
899 Southern Ocean waters, *Nature*, 407, 695-702, 2000a.

900 Boyd, P. W., LaRoche, J., Gall, M. P., Frew, R., and McKay, R. M. L.: Role of iron, light, and  
901 silicate in controlling algal biomass in subantarctic waters SE of New Zealand, *Journal of  
902 Geophysical Research: Oceans*, 104, 13395-13408, 10.1029/1999JC900009, 1999.

903 Boyd, P. W., Watson, A. J., Law, C. S., Abraham, E. R., Trull, T., Murdoch, R., Bakker, D. C. E.,  
904 Bowie, A. R., Buesseler, K. O., Chang, H., Charette, M., Croot, P., Downing, K., Frew, R., Gall, M.,  
905 Hadfield, M., Hall, J., Harvey, M., Jameson, G., LaRoche, J., Liddicoat, M., Ling, R., Maldonado,  
906 M. T., McKay, R. M., Nodder, S., Pickmere, S., Pridmore, R., Rintoul, S., Safi, K., Sutton, P.,  
907 Strzepek, R., Tanneberger, K., Turner, S., Waite, A., and Zeldis, J.: A mesoscale phytoplankton  
908 bloom in the polar Southern Ocean stimulated by iron fertilization, *Nature*, 407, 695-702,  
909 2000b.

910 Boyd, P. W., and Trull, T. W.: Understanding the export of biogenic particles in oceanic waters:  
911 Is there consensus?, *Progress in Oceanography*, 72, 276-312,  
912 <http://dx.doi.org/10.1016/j.pocean.2006.10.007>, 2007.

913 Boyd, P. W., Strzepek, R., Fu, F., and Hutchins, D. A.: Environmental control of open-ocean  
914 phytoplankton groups: Now and in the future, *Limnology and Oceanography*, 55, 1353-1376,  
915 10.4319/lo.2010.55.3.1353, 2010.

916 Brand, L. E., Sunda, W. G., and Guillard, R. R. L.: Limitation of marine phytoplankton  
917 reproductive rates by zinc, manganese, and iron1, *Limnology and Oceanography*, 28, 1182-  
918 1198, 10.4319/lo.1983.28.6.1182, 1983.

919 Brzezinski, M. A., Nelson, D. M., Franck, V. M., and Sigmon, D. E.: Silicon dynamics within an  
920 intense open-ocean diatom bloom in the Pacific sector of the Southern Ocean, *Deep Sea*  
921 *Research Part II: Topical Studies in Oceanography*, 48, 3997-4018,  
922 [http://dx.doi.org/10.1016/S0967-0645\(01\)00078-9](http://dx.doi.org/10.1016/S0967-0645(01)00078-9), 2001.

923 Buesseler, K. O., Antia, A. N., Chen, M., Fowler, S. W., Gardner, W. D., Gustafsson, O., Harada,  
924 K., Michaels, A. F., der Loeff, M. R. v., and Sarin, M.: An assessment of the use of sediment  
925 traps for estimating upper ocean particle fluxes, *Journal of Marine Research*, 65, 345-416, 2007.

926 CARINA, g.: Temperature, salinity, nutrients, carbon, and other profile data collected  
927 worldwide as part of the CARINA project (NODC Accession 0057766). Version 2.2.,  
928 10.3334/CDIAC/OTG.NDP091, 2011.

929 Cermeño, P., Dutkiewicz, S., Harris, R. P., Follows, M., Schofield, O., and Falkowski, P. G.: The  
930 role of nutricline depth in regulating the ocean carbon cycle, *Proceedings of the National*  
931 *Academy of Sciences*, 105, 20344-20349, 10.1073/pnas.0811302106, 2008.

932 Closset, I., Cardinal, D., Bray, S. G., Thil, F., Djouraev, I., Rigual-Hernández, A. S., and Trull, T.  
933 W.: Seasonal variations, origin, and fate of settling diatoms in the Southern Ocean tracked by  
934 silicon isotope records in deep sediment traps, *Global Biogeochemical Cycles*, 29, 1495-1510,  
935 10.1002/2015GB005180, 2015.

936 Cook, S. S., Whittock, L., Wright, S. W., and Hallegraeff, G. M.: Photosynthetic pigment and  
937 genetic differences between two southern ocean morphotypes of *Emiliana huxleyi*  
938 (haptophyta), *Journal of phycology*, 47, 615-626, 2011.

939 Cook, S. S., Jones, R. C., Vaillancourt, R. E., and Hallegraeff, G. M.: Genetic differentiation  
940 among Australian and Southern Ocean populations of the ubiquitous coccolithophore  
941 *Emiliana huxleyi* (Haptophyta), *Phycologia*, 52, 368-374, 10.2216/12-111.1, 2013.

942 Cubillos, J., Wright, S., Nash, G., De Salas, M., Griffiths, B., Tilbrook, B., Poisson, A., and  
943 Hallegraeff, G.: Calcification morphotypes of the coccolithophorid *Emiliana huxleyi* in the  
944 Southern Ocean: changes in 2001 to 2006 compared to historical data, *Marine Ecology*  
945 *Progress Series*, 348, 47-54, 2007.

946 Deppeler, S. L., and Davidson, A. T.: Southern Ocean Phytoplankton in a Changing Climate,  
947 *Frontiers in Marine Science*, 4, 10.3389/fmars.2017.00040, 2017.

948 Ebersbach, F., Trull, T. W., Davies, D. M., and Bray, S. G.: Controls on mesopelagic particle  
949 fluxes in the Sub-Antarctic and Polar Frontal Zones in the Southern Ocean south of Australia in  
950 summer—Perspectives from free-drifting sediment traps, *Deep Sea Research Part II: Topical*  
951 *Studies in Oceanography*, 58, 2260-2276, <http://dx.doi.org/10.1016/j.dsr2.2011.05.025>, 2011.

952 Falkowski, P. G., Katz, M. E., Knoll, A. H., Quigg, A., Raven, J. A., Schofield, O., and Taylor, F. J.  
953 R.: The Evolution of Modern Eukaryotic Phytoplankton, *Science*, 305, 354-360,  
954 10.1126/science.1095964, 2004.

955 Feely, R. A., Doney, S. C., and Cooley, S. R.: Ocean acidification: present conditions and future  
956 changes in a high-CO<sub>2</sub> world, 2009.

957 Feng, Y., Roleda, M. Y., Armstrong, E., Boyd, P. W., and Hurd, C. L.: Environmental controls on  
958 the growth, photosynthetic and calcification rates of a Southern Hemisphere strain of the  
959 coccolithophore *Emiliana huxleyi*, *Limnology and Oceanography*, 62, 519-540,  
960 10.1002/lno.10442, 2017.

961 Fetterer, F., Knowles, K., Meier, W., Savoie, M., and Windnagel, A. K.: Sea Ice Index, Version 3  
962 [Sea Ice Extent], <http://dx.doi.org/10.7265/N5K072F8>, 2017.

963 Flores, J. A., and Sierro, F. J.: A revised technique for the calculation of calcareous nannofossil  
964 accumulation rates., *Micropaleontology*, 43, 321-324, 1997.

965 Freeman, N. M., and Lovenduski, N. S.: Decreased calcification in the Southern Ocean over the  
966 satellite record, *Geophysical Research Letters*, 42, 1834-1840, 10.1002/2014GL062769, 2015.

967 Frölicher, T. L., Sarmiento, J. L., Paynter, D. J., Dunne, J. P., Krasting, J. P., and Winton, M.:  
968 Dominance of the Southern Ocean in Anthropogenic Carbon and Heat Uptake in CMIP5  
969 Models, *Journal of Climate*, 28, 862-886, 10.1175/jcli-d-14-00117.1, 2015.

970 Fuertes, M.-Á., Flores, J.-A., and Sierro, F. J.: The use of circularly polarized light for biometry,  
971 identification and estimation of mass of coccoliths, *Marine Micropaleontology*, 113, 44-55,  
972 <http://dx.doi.org/10.1016/j.marmicro.2014.08.007>, 2014.

973 Gafar, N. A., Eyre, B. D., and Schulz, K. G.: A Conceptual Model for Projecting Coccolithophorid  
974 Growth, Calcification and Photosynthetic Carbon Fixation Rates in Response to Global Ocean  
975 Change, *Frontiers in Marine Science*, 4, 10.3389/fmars.2017.00433, 2018.

976 Gal, A., Wirth, R., Kopka, J., Fratzl, P., Faivre, D., and Scheffel, A.: Macromolecular recognition  
977 directs calcium ions to coccolith mineralization sites, *Science*, 353, 590-593,  
978 10.1126/science.aaf7889, 2016.

979 Giraudeau, J., and Beaufort, L.: Coccolithophores: from extant populations to fossil  
980 assemblages, *Proxies in Late Cenozoic paleoceanography—Developments in Marine Geology*,  
981 edited by: Hillaire-Marcel, C. and De Vernal, A., Elsevier, 409-439, 2007.

982 Gladstone, R. M., Bigg, G. R., and Nicholls, K. W.: Iceberg trajectory modeling and meltwater  
983 injection in the Southern Ocean, *Journal of Geophysical Research: Oceans*, 106, 19903-19915,  
984 10.1029/2000JC000347, 2001.

985 Hagino, K., Bendif, E. M., Young, J. R., Kogame, K., Probert, I., Takano, Y., Horiguchi, T., de  
986 Vargas, C., and Okada, H.: New evidence for morphological and genetic variation in the  
987 cosmopolitan coccolithophore *Emiliana huxleyi* (prymnesiophyceae) from the COX1b-ATP4  
988 genes1, *Journal of Phycology*, 47, 1164-1176, 10.1111/j.1529-8817.2011.01053.x, 2011.

989 Hall, J. A., and Safi, K.: The impact of in situ Fe fertilisation on the microbial food web in the  
990 Southern Ocean, *Deep Sea Research Part II: Topical Studies in Oceanography*, 48, 2591-2613,  
991 [https://doi.org/10.1016/S0967-0645\(01\)00010-8](https://doi.org/10.1016/S0967-0645(01)00010-8), 2001.

992 Henderiks, J., Winter, A., Elbrächter, M., Feistel, R., van der Plas, A., Nausch, G., and Barlow, R.:  
993 Environmental controls on *Emiliana huxleyi* morphotypes in the Benguela coastal upwelling  
994 system (SE Atlantic), *Marine Ecology Progress Series*, 448, 51-66, 2012.

995 Holligan, P. M., Viollier, M., Harbour, D. S., Camus, P., and Champagne-Philippe, M.: Satellite  
996 and ship studies of coccolithophore production along a continental shelf edge, *Nature*, 304,  
997 339-342, 1983.

998 Holligan, P. M., Charalampopoulou, A., and Hutson, R.: Seasonal distributions of the  
999 coccolithophore, *Emiliana huxleyi*, and of particulate inorganic carbon in surface waters of the  
1000 Scotia Sea, *Journal of Marine Systems*, 82, 195-205,  
1001 <http://dx.doi.org/10.1016/j.jmarsys.2010.05.007>, 2010.

1002 Honjo, S., and Doherty, K. W.: Large aperture time-series sediment traps; design objectives,  
1003 construction and application, *Deep Sea Research Part A. Oceanographic Research Papers*, 35,  
1004 133-149, 1988.

1005 Hopkins, J., Henson, S. A., Painter, S. C., Tyrrell, T., and Poulton, A. J.: Phenological  
1006 characteristics of global coccolithophore blooms, *Global Biogeochemical Cycles*, 29, 239-253,  
1007 10.1002/2014GB004919, 2015.

1008 Kemp, A. E. S., Pike, J., Pearce, R. B., and Lange, C. B.: The "Fall dump" -- a new perspective on  
1009 the role of a "shade flora" in the annual cycle of diatom production and export flux, *Deep Sea*  
1010 *Research Part II: Topical Studies in Oceanography*, 47, 2129-2154, 2000.

1011 Khatiwala, S., Primeau, F., and Hall, T.: Reconstruction of the history of anthropogenic CO<sub>2</sub>  
1012 concentrations in the ocean, 2009.

1013 Klaas, C., and Archer, D. E.: Association of sinking organic matter with various types of mineral  
1014 ballast in the deep sea: Implications for the rain ratio, *Global Biogeochemical Cycles*, 16, 63-61-  
1015 63-14, 10.1029/2001GB001765, 2002.

1016 Knappertsbusch, M., Cortes, M. Y., and Thierstein, H. R.: Morphologic variability of the  
1017 coccolithophorid *Calcidiscus leptoporus* in the plankton, surface sediments and from the Early  
1018 Pleistocene, *Marine Micropaleontology*, 30, 293-317, [https://doi.org/10.1016/S0377-](https://doi.org/10.1016/S0377-8398(96)00053-9)  
1019 [8398\(96\)00053-9](https://doi.org/10.1016/S0377-8398(96)00053-9), 1997.

1020 Langer, G., and Benner, I.: Effect of elevated nitrate concentration on calcification in *Emiliania*  
1021 *huxleyi*, *Journal of Nannoplankton Research*, 30, 77-80, 2009.

1022 Lee, R. B. Y., Mavridou, D. A. I., Papadakos, G., McClelland, H. L. O., and Rickaby, R. E. M.: The  
1023 uronic acid content of coccolith-associated polysaccharides provides insight into  
1024 coccolithogenesis and past climate, *Nature Communications*, 7, 13144, 10.1038/ncomms13144  
1025 <https://www.nature.com/articles/ncomms13144#supplementary-information>, 2016.

1026 Levitus, S., Antonov, J. I., Boyer, T. P., and Stephens, C.: Warming of the World Ocean, *Science*,  
1027 287, 2225-2229, 10.1126/science.287.5461.2225, 2000.

1028 Litchman, E., Edwards, K. F., Klausmeier, C. A., and Thomas, M. K.: Phytoplankton niches, traits  
1029 and eco-evolutionary responses to global environmental change, *Marine Ecology Progress*  
1030 *Series*, 470, 235-248, 2012.

1031 Locarnini, R. A., Mishonov, A. V., Antonov, J. I., Boyer, T. P., Garcia, H. E., Baranova, O. K.,  
1032 Zweng, M. M., and Johnson, D. R.: *World Ocean Atlas 2009, Volume 1: Temperature*, NOAA  
1033 *Atlas NESDIS 68*, edited by: Levitus, S., U.S. Government Printing Office, Washington, D.C.,  
1034 2010.

1035 Lochte, K., Ducklow, H. W., Fasham, M. J. R., and Stienen, C.: Plankton succession and carbon  
1036 cycling at 47°N 20°W during the JGOFS North Atlantic Bloom Experiment, *Deep Sea Research*  
1037 *Part II: Topical Studies in Oceanography*, 40, 91-114, [http://dx.doi.org/10.1016/0967-](http://dx.doi.org/10.1016/0967-0645(93)90008-B)  
1038 [0645\(93\)90008-B](http://dx.doi.org/10.1016/0967-0645(93)90008-B), 1993.

1039 Lombard, F., da Rocha, R. E., Bijma, J., and Gattuso, J.: Effect of carbonate ion concentration  
1040 and irradiance on calcification in planktonic foraminifera, *Biogeosciences*, 7, 247-255, 2010.

1041 Malinverno, E., Triantaphyllou, M. V., and Dimiza, M. D.: Coccolithophore assemblage  
1042 distribution along a temperate to polar gradient in the West Pacific sector of the Southern  
1043 Ocean (January 2005), *Micropaleontology*, 61, 489-506, 2015.

1044 Margalef, R.: Life-forms of phytoplankton as survival alternatives in an unstable environment,  
1045 *Oceanologica Acta*, 1, 493-509, 1978.

1046 Massom, R., Reid, P., Stammerjohn, S., Raymond, B., Fraser, A., and Ushio, S.: Change and  
1047 Variability in East Antarctic Sea Ice Seasonality, 1979/80-2009/10, *PLOS ONE*, 8, e64756,  
1048 10.1371/journal.pone.0064756, 2013.

1049 McNeil, B. I., and Matear, R. J.: Southern Ocean acidification: A tipping point at 450-ppm  
1050 atmospheric CO<sub>2</sub>, *Proceedings of the National Academy of Sciences*, 105, 18860-18864, 2008.

1051 Meier, K. J. S., Beaufort, L., Heussner, S., and Ziveri, P.: The role of ocean acidification in  
1052 *Emiliania huxleyi* coccolith thinning in the Mediterranean Sea, *Biogeosciences*, 11, 2857-2869,  
1053 10.5194/bg-11-2857-2014, 2014.

1054 Merico, A., Tyrrell, T., Lessard, E. J., Oguz, T., Stabeno, P. J., Zeeman, S. I., and Whitledge, T. E.:  
1055 Modelling phytoplankton succession on the Bering Sea shelf: role of climate influences and

1056 trophic interactions in generating *Emiliana huxleyi* blooms 1997–2000, Deep Sea Research  
1057 Part I: Oceanographic Research Papers, 51, 1803-1826,  
1058 <https://doi.org/10.1016/j.dsr.2004.07.003>, 2004.

1059 Milliman, J. D., Troy, P. J., Balch, W. M., Adams, A. K., Li, Y. H., and Mackenzie, F. T.: Biologically  
1060 mediated dissolution of calcium carbonate above the chemical lysocline?, Deep Sea Research  
1061 Part I: Oceanographic Research Papers, 46, 1653-1669, [http://dx.doi.org/10.1016/S0967-](http://dx.doi.org/10.1016/S0967-0637(99)00034-5)  
1062 [0637\(99\)00034-5](http://dx.doi.org/10.1016/S0967-0637(99)00034-5), 1999.

1063 Moy, A. D., Howard, W. R., Bray, S. G., and Trull, T. W.: Reduced calcification in modern  
1064 Southern Ocean planktonic foraminifera, Nature Geosci, 2, 276-280,  
1065 [http://www.nature.com/ngeo/journal/v2/n4/supinfo/ngeo460\\_S1.html](http://www.nature.com/ngeo/journal/v2/n4/supinfo/ngeo460_S1.html), 2009.

1066 Muggli, D. L., and Harrison, P. J.: Effects of iron on two oceanic phytoplankters grown in  
1067 natural NE subarctic pacific seawater with no artificial chelators present, Journal of  
1068 Experimental Marine Biology and Ecology, 212, 225-237, [http://dx.doi.org/10.1016/S0022-](http://dx.doi.org/10.1016/S0022-0981(96)02752-9)  
1069 [0981\(96\)02752-9](http://dx.doi.org/10.1016/S0022-0981(96)02752-9), 1997.

1070 Orr, J. C., Fabry, V. J., Aumont, O., Bopp, L., Doney, S. C., Feely, R. A., Gnanadesikan, A., Gruber,  
1071 N., Ishida, A., and Joos, F.: Anthropogenic ocean acidification over the twenty-first century and  
1072 its impact on calcifying organisms, Nature, 437, 681-686, 2005.

1073 Orsi, A. H., Whitworth Iii, T., and Nowlin Jr, W. D.: On the meridional extent and fronts of the  
1074 Antarctic Circumpolar Current, Deep Sea Research Part I: Oceanographic Research Papers, 42,  
1075 641-673, [http://dx.doi.org/10.1016/0967-0637\(95\)00021-W](http://dx.doi.org/10.1016/0967-0637(95)00021-W), 1995.

1076 Paasche, E., and Brubak, S.: Enhanced calcification in the coccolithophorid *Emiliana huxleyi*  
1077 (Haptophyceae) under phosphorus limitation, Phycologia, 33, 324-330, 10.2216/i0031-8884-  
1078 33-5-324.1, 1994.

1079 Paasche, E.: Reduced coccolith calcite production under light-limited growth: a comparative  
1080 study of three clones of *Emiliana huxleyi* (Prymnesiophyceae), Phycologia, 38, 508-516,  
1081 10.2216/i0031-8884-38-6-508.1, 1999.

1082 Paasche, E.: A review of the coccolithophorid *Emiliana huxleyi* (Prymnesiophyceae), with  
1083 particular reference to growth, coccolith formation, and calcification-photosynthesis  
1084 interactions, Phycologia, 40, 503-529, 10.2216/i0031-8884-40-6-503.1, 2002.

1085 Pardo, P. C., Tilbrook, B., Langlais, C., Trull, T. W., and Rintoul, S. R.: Carbon uptake and  
1086 biogeochemical change in the Southern Ocean, south of Tasmania, Biogeosciences, 14, 5217-  
1087 5237, 10.5194/bg-14-5217-2017, 2017.

1088 Parslow, J. S., Boyd, P. W., Rintoul, S. R., and Griffiths, F. B.: A persistent subsurface chlorophyll  
1089 maximum in the Interpolar Frontal Zone south of Australia: Seasonal progression and  
1090 implications for phytoplankton-light-nutrient interactions, Journal of Geophysical Research:  
1091 Oceans, 106, 31543-31557, 10.1029/2000JC000322, 2001.

1092 Passow, U., and De La Rocha, C. L.: Accumulation of mineral ballast on organic aggregates,  
1093 Global Biogeochemical Cycles, 20, GB1013, 10.1029/2005GB002579, 2006.

1094 Patil, S. M., Mohan, R., Shetye, S. S., Gazi, S., Baumann, K.-H., and Jafar, S.: Biogeographic  
1095 distribution of extant Coccolithophores in the Indian sector of the Southern Ocean, Marine  
1096 Micropaleontology, 137, 16-30, <https://doi.org/10.1016/j.marmicro.2017.08.002>, 2017.

1097 Poulton, A. J., Young, J. R., Bates, N. R., and Balch, W. M.: Biometry of detached *Emiliana*  
1098 *huxleyi* coccoliths along the Patagonian Shelf, Marine Ecology Progress Series, 443, 1-17, 2011.

1099 Quéguiner, B.: Iron fertilization and the structure of planktonic communities in high nutrient  
1100 regions of the Southern Ocean, Deep Sea Research Part II: Topical Studies in Oceanography,  
1101 90, 43-54, <http://dx.doi.org/10.1016/j.dsr2.2012.07.024>, 2013.

1102 Rembauville, M., Meilland, J., Ziveri, P., Schiebel, R., Blain, S., and Salter, I.: Planktic foraminifer  
1103 and coccolith contribution to carbonate export fluxes over the central Kerguelen Plateau, Deep  
1104 Sea Research Part I: Oceanographic Research Papers, 111, 91-101,  
1105 <http://dx.doi.org/10.1016/j.dsr.2016.02.017>, 2016.

1106 Reynolds, R. W., Rayner, N. A., Smith, T. M., Stokes, D. C., and Wang, W.: An Improved In Situ  
1107 and Satellite SST Analysis for Climate, *Journal of Climate*, 15, 1609-1625, 10.1175/1520-  
1108 0442(2002)015<1609:aiisas>2.0.co;2, 2002.

1109 Ridgwell, A., and Zeebe, R. E.: The role of the global carbonate cycle in the regulation and  
1110 evolution of the Earth system, *Earth and Planetary Science Letters*, 234, 299-315,  
1111 <https://doi.org/10.1016/j.epsl.2005.03.006>, 2005.

1112 Rigual-Hernández, A. S., Trull, T. W., Bray, S. G., Closset, I., and Armand, L. K.: Seasonal  
1113 dynamics in diatom and particulate export fluxes to the deep sea in the Australian sector of  
1114 the southern Antarctic Zone, *Journal of Marine Systems*, 142, 62-74,  
1115 <http://dx.doi.org/10.1016/j.jmarsys.2014.10.002>, 2015a.

1116 Rigual-Hernández, A. S., Trull, T. W., Bray, S. G., Cortina, A., and Armand, L. K.: Latitudinal and  
1117 temporal distributions of diatom populations in the pelagic waters of the Subantarctic and  
1118 Polar Frontal Zones of the Southern Ocean and their role in the biological pump,  
1119 *Biogeosciences* 12, 8615-8690, 10.5194/bgd-12-8615-2015, 2015b.

1120 Rost, B., and Riebesell, U.: Coccolithophores and the biological pump: responses to  
1121 environmental changes, in: *Coccolithophores: From Molecular Processes to Global Impact*,  
1122 edited by: Thierstein, H. R., and Young, J. R., Springer Berlin Heidelberg, Berlin, Heidelberg, 99-  
1123 125, 2004.

1124 Saavedra-Pellitero, M., Baumann, K.-H., Flores, J.-A., and Gersonde, R.: Biogeographic  
1125 distribution of living coccolithophores in the Pacific sector of the Southern Ocean, *Marine*  
1126 *Micropaleontology*, 109, 1-20, 2014.

1127 Salter, I., Schiebel, R., Ziveri, P., Movellan, A., Lampitt, R., and Wolff, G. A.: Carbonate counter  
1128 pump stimulated by natural iron fertilization in the Polar Frontal Zone, *Nature Geosci*, 7, 885-  
1129 889, 10.1038/ngeo2285

1130 [http://www.nature.com/ngeo/journal/v7/n12/abs/ngeo2285.html#supplementary-](http://www.nature.com/ngeo/journal/v7/n12/abs/ngeo2285.html#supplementary-information)  
1131 [information](http://www.nature.com/ngeo/journal/v7/n12/abs/ngeo2285.html#supplementary-information), 2014.

1132 Sarmiento, J. L., Gruber, N., Brzezinski, M. A., and Dunne, J. P.: High-latitude controls of  
1133 thermocline nutrients and low latitude biological productivity, *Nature*, 427, 56-60, 2004a.

1134 Sarmiento, J. L., Slater, R., Barber, R., Bopp, L., Doney, S. C., Hirst, A. C., Kleypas, J., Matear, R.,  
1135 Mikolajewicz, U., Monfray, P., Soldatov, V., Spall, S. A., and Stouffer, R.: Response of ocean  
1136 ecosystems to climate warming, *Global Biogeochemical Cycles*, 18, n/a-n/a,  
1137 10.1029/2003GB002134, 2004b.

1138 Saruwatari, K., Satoh, M., Harada, N., Suzuki, I., and Shiraiwa, Y.: Change in coccolith size and  
1139 morphology due to response to temperature and salinity in coccolithophore *Emiliania huxleyi*  
1140 (Haptophyta) isolated from the Bering and Chukchi seas, *Biogeosciences*, 13, 2743-2755,  
1141 10.5194/bg-13-2743-2016, 2016.

1142 Schulz, K., Zondervan, I., Gerringa, L., Timmermans, K., Veldhuis, M., and Riebesell, U.: Effect of  
1143 trace metal availability on coccolithophorid calcification, *Nature*, 430, 673-676, 2004.

1144 Siegel, D. A., and Deuser, W. G.: Trajectories of sinking particles in the Sargasso Sea: modeling  
1145 of statistical funnels above deep-ocean sediment traps, *Deep Sea Research Part I:*  
1146 *Oceanographic Research Papers*, 44, 1519-1541, [http://dx.doi.org/10.1016/S0967-](http://dx.doi.org/10.1016/S0967-0637(97)00028-9)  
1147 [0637\(97\)00028-9](http://dx.doi.org/10.1016/S0967-0637(97)00028-9), 1997.

1148 Siegel, D. A., Fields, E., and Buesseler, K. O.: A bottom-up view of the biological pump:  
1149 Modeling source funnels above ocean sediment traps, *Deep Sea Research Part I:*  
1150 *Oceanographic Research Papers*, 55, 108-127, <http://dx.doi.org/10.1016/j.dsr.2007.10.006>,  
1151 2008.

1152 Sieracki, M. E., Verity, P. G., and Stoecker, D. K.: Plankton community response to sequential  
1153 silicate and nitrate depletion during the 1989 North Atlantic spring bloom, *Deep Sea Research*  
1154 *Part II: Topical Studies in Oceanography*, 40, 213-225, [http://dx.doi.org/10.1016/0967-](http://dx.doi.org/10.1016/0967-0645(93)90014-E)  
1155 [0645\(93\)90014-E](http://dx.doi.org/10.1016/0967-0645(93)90014-E), 1993.

1156 Sigman, D. M., and Boyle, E. A.: Glacial/interglacial variations in atmospheric carbon dioxide,  
1157 Nature, 407, 859-869, 2000.

1158 Smith, H. E. K., Tyrrell, T., Charalampopoulou, A., Dumousseaud, C., Legge, O. J., Birchenough,  
1159 S., Pettit, L. R., Garley, R., Hartman, S. E., Hartman, M. C., Sagoo, N., Daniels, C. J., Achterberg,  
1160 E. P., and Hydes, D. J.: Predominance of heavily calcified coccolithophores at low CaCO<sub>3</sub>  
1161 saturation during winter in the Bay of Biscay, Proceedings of the National Academy of  
1162 Sciences, 109, 8845-8849, [10.1073/pnas.1117508109](https://doi.org/10.1073/pnas.1117508109), 2012.

1163 Sohrin, Y., Iwamoto, S., Matsui, M., Obata, H., Nakayama, E., Suzuki, K., Handa, N., and Ishii,  
1164 M.: The distribution of Fe in the Australian sector of the Southern Ocean, Deep Sea Research  
1165 Part I: Oceanographic Research Papers, 47, 55-84, [https://doi.org/10.1016/S0967-](https://doi.org/10.1016/S0967-0637(99)00049-7)  
1166 [0637\(99\)00049-7](https://doi.org/10.1016/S0967-0637(99)00049-7), 2000.

1167 Tagliabue, A., Sallee, J.-B., Bowie, A. R., Levy, M., Swart, S., and Boyd, P. W.: Surface-water iron  
1168 supplies in the Southern Ocean sustained by deep winter mixing, Nature Geosci, 7, 314-320,  
1169 [10.1038/ngeo2101](https://doi.org/10.1038/ngeo2101)

1170 [http://www.nature.com/ngeo/journal/v7/n4/abs/ngeo2101.html#supplementary-](http://www.nature.com/ngeo/journal/v7/n4/abs/ngeo2101.html#supplementary-information)  
1171 [information](http://www.nature.com/ngeo/journal/v7/n4/abs/ngeo2101.html#supplementary-information), 2014.

1172 Takahashi, T., Sutherland, S. C., Wanninkhof, R., Sweeney, C., Feely, R. A., Chipman, D. W.,  
1173 Hales, B., Friederich, G., Chavez, F., Sabine, C., Watson, A., Bakker, D. C. E., Schuster, U., Metzl,  
1174 N., Yoshikawa-Inoue, H., Ishii, M., Midorikawa, T., Nojiri, Y., Körtzinger, A., Steinhoff, T.,  
1175 Hoppema, M., Olafsson, J., Arnarson, T. S., Tilbrook, B., Johannessen, T., Olsen, A., Bellerby, R.,  
1176 Wong, C. S., Delille, B., Bates, N. R., and de Baar, H. J. W.: Climatological mean and decadal  
1177 change in surface ocean pCO<sub>2</sub>, and net sea-air CO<sub>2</sub> flux over the global oceans, Deep Sea  
1178 Research Part II: Topical Studies in Oceanography, 56, 554-577,  
1179 <https://doi.org/10.1016/j.dsr2.2008.12.009>, 2009.

1180 Thunell, R., Pride, C., Ziveri, P., Muller-Karger, F., Sancetta, C., and Murray, D.: Plankton  
1181 response to physical forcing in the Gulf of California, Journal of Plankton Research, 18, 2017-  
1182 2026, [10.1093/plankt/18.11.2017](https://doi.org/10.1093/plankt/18.11.2017), 1996.

1183 Trull, T. W., Bray, S. G., Manganini, S. J., Honjo, S., and François, R.: Moored sediment trap  
1184 measurements of carbon export in the Subantarctic and Polar Frontal zones of the Southern  
1185 Ocean, south of Australia, Journal of Geophysical Research: Oceans, 106, 31489-31509,  
1186 [10.1029/2000JC000308](https://doi.org/10.1029/2000JC000308), 2001a.

1187 Trull, T. W., Rintoul, S. R., Hadfield, M., and Abraham, E. R.: Circulation and seasonal evolution  
1188 of polar waters south of Australia: implications for iron fertilization of the Southern Ocean,  
1189 Deep Sea Research Part II: Topical Studies in Oceanography, 48, 2439-2466,  
1190 [http://dx.doi.org/10.1016/S0967-0645\(01\)00003-0](http://dx.doi.org/10.1016/S0967-0645(01)00003-0), 2001b.

1191 Trull, T. W., Sedwick, P. N., Griffiths, F. B., and Rintoul, S. R.: Introduction to special section:  
1192 SAZ Project, Journal of Geophysical Research: Oceans, 106, 31425-31429,  
1193 [10.1029/2001JC001008](https://doi.org/10.1029/2001JC001008), 2001c.

1194 Trull, T. W., Passmore, A., Davies, D. M., Smit, T., Berry, K., and Tilbrook, B.: The distribution of  
1195 pelagic biogenic carbonates in the Southern Ocean south of Australia: a baseline for ocean  
1196 acidification impact assessment, Biogeosciences, in press, 2017.

1197 Turner, J. T.: Zooplankton fecal pellets, marine snow and sinking phytoplankton blooms,  
1198 Aquatic Microbial Ecology, 27, 57-102, 2002.

1199 Turner, J. T.: Zooplankton fecal pellets, marine snow, phytodetritus and the ocean's biological  
1200 pump, Progress in Oceanography, 130, 205-248,  
1201 <http://dx.doi.org/10.1016/j.pocean.2014.08.005>, 2015.

1202 Wilks, J. V., Rigual-Hernández, A. S., Trull, T. W., Bray, S. G., Flores, J.-A., and Armand, L. K.:  
1203 Biogeochemical flux and phytoplankton succession: A year-long sediment trap record in the  
1204 Australian sector of the Subantarctic Zone, Deep Sea Research Part I: Oceanographic Research  
1205 Papers, 121, 143-159, <https://doi.org/10.1016/j.dsr.2017.01.001>, 2017.

1206 Winter, A., Henderiks, J., Beaufort, L., Rickaby, R. E., and Brown, C. W.: Poleward expansion of  
1207 the coccolithophore *Emiliana huxleyi*, *Journal of Plankton Research*, 36, 316-325, 2014.  
1208 Young, J., Geisen, M., Cross, L., Kleijne, A., Sprengel, C., Probert, I., and Østergaard, J.: A guide  
1209 to extant coccolithophore taxonomy, *Journal of Nanoplankton Research Special Issue 1*,  
1210 International Nannoplankton Association, 2003.  
1211 Young, J. R., and Westbroek, P.: Genotypic variation in the coccolithophorid species *Emiliana*  
1212 *huxleyi*, *Marine Micropaleontology*, 18, 5-23, [https://doi.org/10.1016/0377-8398\(91\)90004-P](https://doi.org/10.1016/0377-8398(91)90004-P),  
1213 1991.  
1214 Young, J. R., and Ziveri, P.: Calculation of coccolith volume and its use in calibration of carbonate  
1215 flux estimates, *Deep Sea Research Part II: Topical Studies in Oceanography*, 47, 1679-1700,  
1216 [http://dx.doi.org/10.1016/S0967-0645\(00\)00003-5](http://dx.doi.org/10.1016/S0967-0645(00)00003-5), 2000.  
1217 Zeebe, R. E.: History of Seawater Carbonate Chemistry, Atmospheric CO<sub>2</sub>, and Ocean  
1218 Acidification, *Annual Review of Earth and Planetary Sciences*, 40, 141-165, 10.1146/annurev-  
1219 earth-042711-105521, 2012.  
1220 Zeldis, J.: Mesozooplankton community composition, feeding, and export production during  
1221 SOIREE, *Deep Sea Research Part II: Topical Studies in Oceanography*, 48, 2615-2634,  
1222 [https://doi.org/10.1016/S0967-0645\(01\)00011-X](https://doi.org/10.1016/S0967-0645(01)00011-X), 2001.  
1223 Zhang, X., Lewis, M., Lee, M., Johnson, B., and Korotaev, G.: The volume scattering function of  
1224 natural bubble populations, *Limnology and Oceanography*, 47, 1273-1282, 2002.  
1225 Zondervan, I.: The effects of light, macronutrients, trace metals and CO<sub>2</sub> on the production of  
1226 calcium carbonate and organic carbon in coccolithophores—A review, *Deep Sea Research Part*  
1227 *II: Topical Studies in Oceanography*, 54, 521-537,  
1228 <http://dx.doi.org/10.1016/j.dsr2.2006.12.004>, 2007.

1229